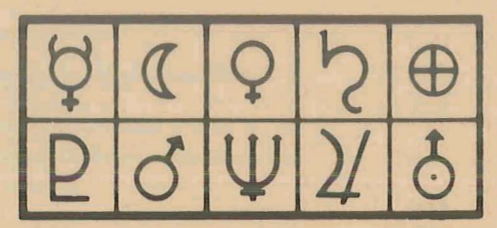

PLANETARY QUARANTINE

QR 18
September 1970

SANDIA LABORATORIES QUARTERLY REPORT
PLANETARY QUARANTINE PROGRAM

Prepared by:
Planetary Quarantine Department 1740

SANDIA LABORATORIES

OPERATED FOR THE U. S. ATOMIC ENERGY COMMISSION BY SANDIA CORPORATION | ALBUQUERQUE, NEW MEXICO; LIVERMORE, CALIFORNIA

Issued by Sandia Corporation,
a prime contractor to the
United States Atomic Energy Commission

SANDIA LABORATORIES QUARTERLY REPORT - PLANETARY QUARANTINE PROGRAM

EIGHTEENTH QUARTERLY REPORT OF PROGRESS

for

Period Ending September 30, 1970

Planetary Quarantine Department
Sandia Laboratories, Albuquerque, New Mexico

September 1970

Project No. 0064010

This work was conducted under Contract No. W-12,853, Bioscience Division, Office of Space Science and Applications, NASA Headquarters, Washington, D. C.

CONTENTS

SANDIA LABORATORIES QUARTERLY REPORT
PLANETARY QUARANTINE PROGRAM

Summary of Activities

Thermoradiation Sterilization. Activities this quarter included an appraisal of the overall thermoradiation program along with considerable experimentation in dry heat, radiation and thermoradiation inactivation of B. subtilis var. niger. Heat resistance and dose rate sensitivity experiments at 95°C revealed promising results at that temperature. At a dose rate of 12 krads/hour, the D value was two hours. A 10 log population reduction could then be accomplished at 95°C with a total dose of less than 250 krads in 20 hours. Good confirmation was also obtained in the dose rate sensitivity of radiation inactivation at room temperature. High rate gamma radiation inactivation at room temperature required twice the total dose that low rate radiation required.

Modeling of Thermoradiation Synergism. Progress this quarter was made in several areas. Among them:

1. Based upon more recent and complete data at ambient temperature (25°C), the model parameter values were recomputed several ways. Generally, the new values represent only small changes from those previously obtained.
2. The trade-offs between radiation dose, dose rate, and temperature were more fully investigated. These trade-offs are presented here for a required 8 log reduction in expected spore population.

For example, for a maximum dose of 150 krad, and a maximum sterilization time of five hours, the optimal sterilization temperature/dose rate combination is about 110°C at 30 krads per hour. By permitting the sterilization cycle to last 8 hours, the same effect may be achieved at about 105°C and a dose rate of about 19 krad/hour.

3. The model has been extended theoretically to include a kinetic representation of the free radical population rather than a birth-and-death process approach. This generalization appears to have the potential of "explaining" experimentally observed phenomena which heretofore were unexplicable.

Thermoradiation Inactivation in Open and Closed Systems. As might be expected, differences have been observed in bacterial spore inactivation rate in open and closed aluminum systems in thermoradiative environments. These differences have been observed at three temperatures above 100°C, and they parallel the behavior of exposed (open) and encapsulated (closed) spores. To attempt to explain these differences, it was assumed that pressure was the variable factor, and the reasonableness of this assumption was then established analytically using the thermoradiation model. It was found that for pressure to be the cause of the differences in inactivation rates between open and closed systems, the activation volume associated with the inactivating reaction must be only a 0.0097% change in the molar volume of DNA. This number was comparable with percentage changes experimentally observed for smaller molecules undergoing chemical reactions.

Preliminary Analysis of the Radiation Burden of a Typical Mars Lander. Post launch a Martian Lander would sustain radiation doses of various types from several sources. In order to determine "safe" levels of radiation for thermoradiation sterilization processes, one needs at least an upper bound on the amount (dose) of radiation encountered post launch. A very "safe" upper bound of about 6300 krads is derived here. This figure is based on an 18 month active life and minimal shielding from the biobarrier.

Humidity Control Systems. The study of spore inactivation at low relative humidities requires a responsive and reliable humidity control system. The controlled saturation temperature system described last quarter was modified by pressurizing the saturation portion of the system and by adding a desiccant bed. These features may be used singly or in combination to deliver air with a relative humidity as low as 0.0035% at 105°C. Both of these modifications and related progress are described in this report.

Bioburden Modeling and Experimentation. Emphasis this quarter has been placed on experimental verification of the estimation and prediction model that has been developed and reported on previously. A promising approach to predictable (and measureable) particle removal from surfaces has been found. This method uses the vacuum probe at subcritical air flow velocities. It was then coupled with the previously developed techniques for particle deposition to obtain plateauing particle burden data. Additional progress has been made toward the predictable tagging of particles with organisms and some preliminary data obtained.

Lunar Planetary Quarantine Information System. This past quarter, the lunar planetary quarantine information system, as it actually exists and

is being used, was documented. In addition, the computerized identification program was completed and a report is in preparation.

Thermoradiation Sterilization

A. Description. The objective of this activity is to thoroughly investigate the sterilizing effects of combinations of heat and radiation, and to assess the practicality of this process for spacecraft sterilization. Thermoradiation offers the possibility of sterilization at temperatures less than 100°C at low dose rates of approximately 10 krad/hour. This is possible because of a synergistic effect in bacterial inactivation which has been observed when combinations of heat and gamma radiation are applied simultaneously. Should any spacecraft components prove to be heat sensitive at high temperatures, thermoradiation offers a potential means of overcoming reliability problems.

There appear to be potentially significant spin-off possibilities for the thermoradiation process in the sterilization of drugs, pharmaceuticals, cosmetics, medical products and food. This is particularly true at the lower temperatures.

B. Progress.

1. Program Planning. A reappraisal of the overall thermoradiation program was made to determine the thoroughness of completed work and that which is planned. [The program has a number of aspects which must be considered in order to establish the feasibility of thermoradiation for spacecraft sterilization. These are, for example, the inactivation with thermoradiation as compared to dry heat and

radiation separately, the effects of water activity, encapsulation, mated surfaces, oxygen tension, etc.]. These various aspects of the study were ordered with respect to the program significance and, planned experiments were defined to give the desired level of model verification. The additional experimentation required will address the following:

a. Additional surface experiments in air are needed using Bacillus subtilis var. niger for model verification to give a full range of temperature/radiation level options. These will be radiation, dry heat and thermoradiation experiments to permit evaluation of thermoradiation with respect to individual heat and radiation effects.

b. Surface experiments in nitrogen are needed to establish the relationship between thermoradiation inactivation and an N_2 environment as compared to inactivation in air. Present plans for terminal dry heat sterilization will use an N_2 atmosphere.

c. A number of additional surface experiments will be needed using other heat and radiation resistant organisms. These will at least include B. stearothermophilus, B. pumilus, S. faecium and some thermophilic organisms.

d. The investigation of radiation, heat and thermoradiation effects in methylmethacrylate will be continued.

e. A few sample experiments with spores encapsulated in epoxy will be needed to tie into the methacrylate work.

f. Mated surface effects - we need to consider thermoradiation sterilization effectiveness on mated surfaces. This configuration, resulting in D values about twice the surface D values, seems to be the basis that will set terminal spacecraft sterilization cycles instead of the encapsulated contamination. The present rationale suggests that all encapsulated contamination will be sterilized during the flight qualification cycle and only surface contamination that accumulates during assembly need be sterilized. Thus the surface contamination that ends in a mated surface condition will be the most difficult to eliminate. We hope to assess this aspect by taking advantage of the techniques that have been developed in the NASA dry heat studies of mated surface sterilization.

2. Experimental Progress. Activities this quarter were devoted primarily to low temperature/low dose rate sterilization. In order to evaluate thermoradiation synergism, it was necessary to establish good base line data for radiation effects over a wide range of dose rates at room temperature. We completed room temperature radiation experiments at dose rates of 2 krads/hour, 4 krads/hour, 8 krads/hour, 34 krads/hour, 51 krads/hour, 120 krads/hour, and 675 krads/hour. These varied in exposure times from 7 days at the low dose rates to 60 minutes at the highest dose rates. Dose rate sensitivity was confirmed even at room temperature. The D value varied from 65 krads (per log population reduction) for the lowest dose rate to 100 krads at the highest

dose rate. The results of room temperature radiation effects are shown in Figures 1 through Figure 7. This data is summarized in Figure 8. (The dose rate sensitivity becomes more pronounced as the temperature increases above room temperature).

An additional requirement to evaluate thermoradiation synergism is to obtain base line dry heat data. We have completed one experiment on B. subtilis at 95°C. The resulting D value from Figure 9 is 12 hours.

We completed a series of thermoradiation experiments at 95°C over a range of gamma dose rates of 6 krads/hour (Figure 10), 11 krads/hour (Figure 11) and 38 krads/hour (Figure 12). The resulting D values were 3.9 hours at 6 krads/hour, 2.3 hours at 11 krads/hour and 0.9 hours at 38 krads/hour. These data are summarized in Figure 13. We plan to be rather thorough at 95°C because of the potential at this temperature. From Figure 13, a D value of 2 hours is available at a dose rate of 11 to 12 krads/hour. This rate would result in a total dose of less than 250 krads for a 10 log population reduction. In addition, sterilization at 95°C would afford many benefits, particularly in the sterilization of spacecraft with life detection and other science packages containing liquids or heat sensitive components.

Figure 14 demonstrates the singular effects of dry heat at 95°C, radiation at 11 krads/hour, and then compares these singular effects to thermoradiation at these same conditicns. A good degree of synergism exists at these conditions as is shown in Figure 14.

The results one would expect if the effects of heat and radiation were additive only are shown as the additive curve. The difference between this additive curve and the the thermoradiation line is due to synergistic inactivation.

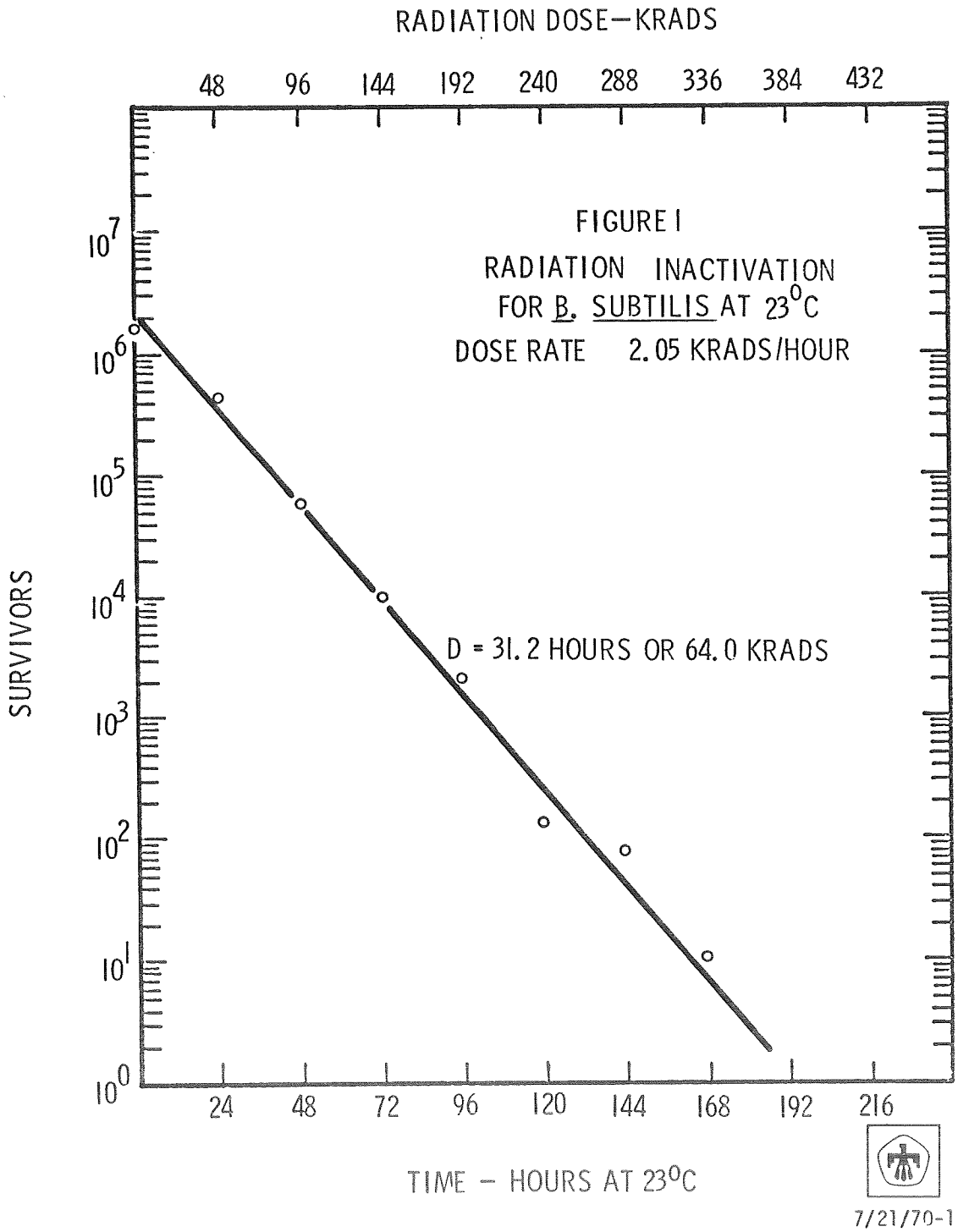
RADIATION DOSE—KRADS
48
96
144
192
240
288
336
384
432
FIGURE I
RADIATION INACTIVATION
FOR B. SUBTILIS AT 23°C
DOSE RATE 2.05 KRADS/HOUR
D = 31.2 HOURS OR 64.0 KRADS
SURVIVORS
10^7
10^6
10^5
10^4
10^3
10^2
10^1
10^0
24
48
72
96
120
144
168
192
216
TIME - HOURS AT 23°C
7/21/70-1

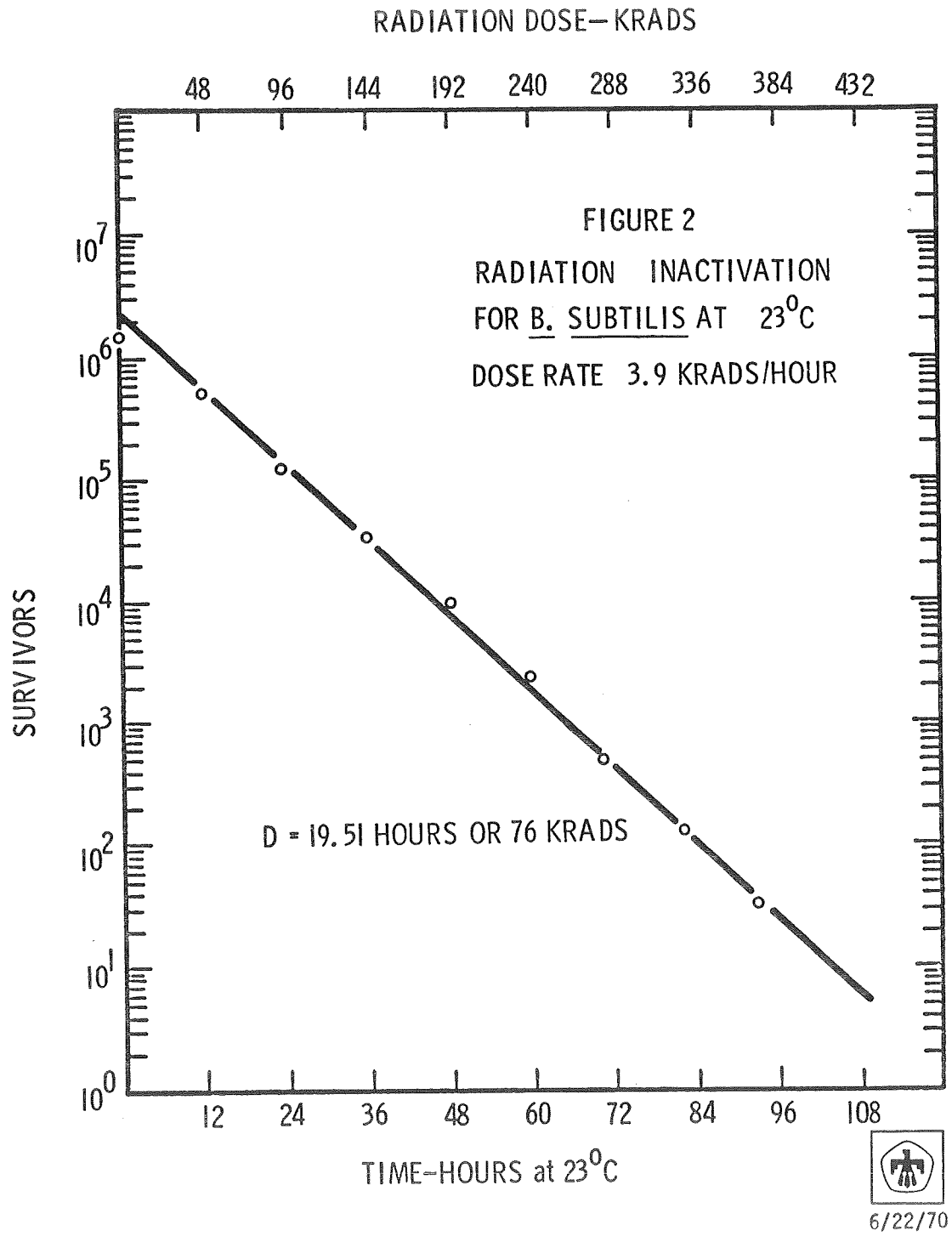
RADIATION DOSE—KRADS
48
96
144
192
240
288
336
384
432
FIGURE 2
RADIATION INACTIVATION
FOR B. SUBTILIS AT 23°C
DOSE RATE 3.9 KRADS/HOUR
SURVIVORS
10^7
10^6
10^5
10^4
10^3
10^2
10^1
10^0
D = 19.51 HOURS OR 76 KRADS
12
24
36
48
60
72
84
96
108
TIME-HOURS at 23°C
6/22/70

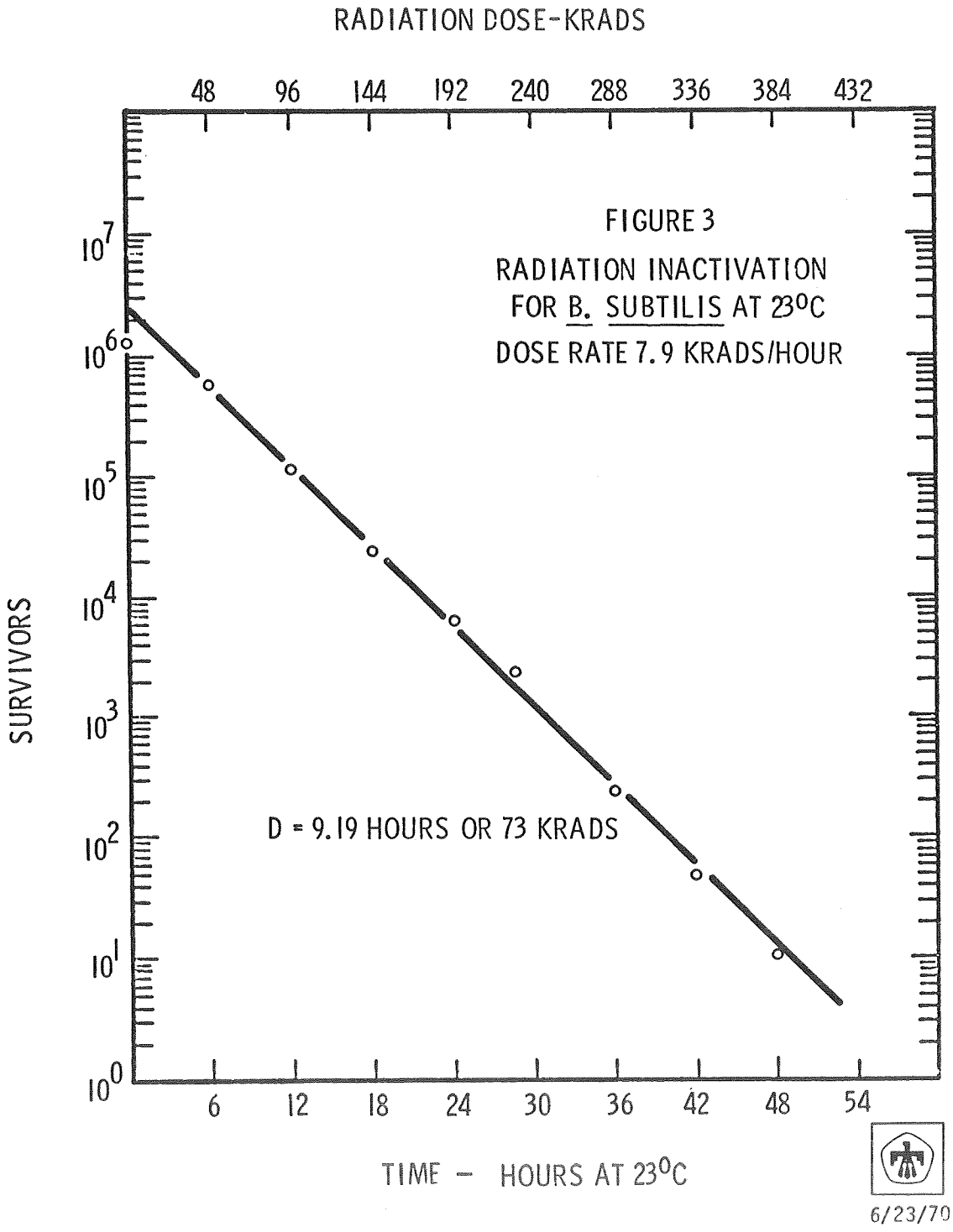
RADIATION DOSE-KRADS
48
96
144
192
240
288
336
384
432
FIGURE 3
RADIATION INACTIVATION
FOR B. SUBTILIS AT 23°C
DOSE RATE 7.9 KRADS/HOUR
SURVIVORS
10^7
10^6
10^5
10^4
10^3
10^2
10^1
10^0
D = 9.19 HOURS OR 73 KRADS
6
12
18
24
30
36
42
48
54
TIME – HOURS AT 23°C
6/23/70

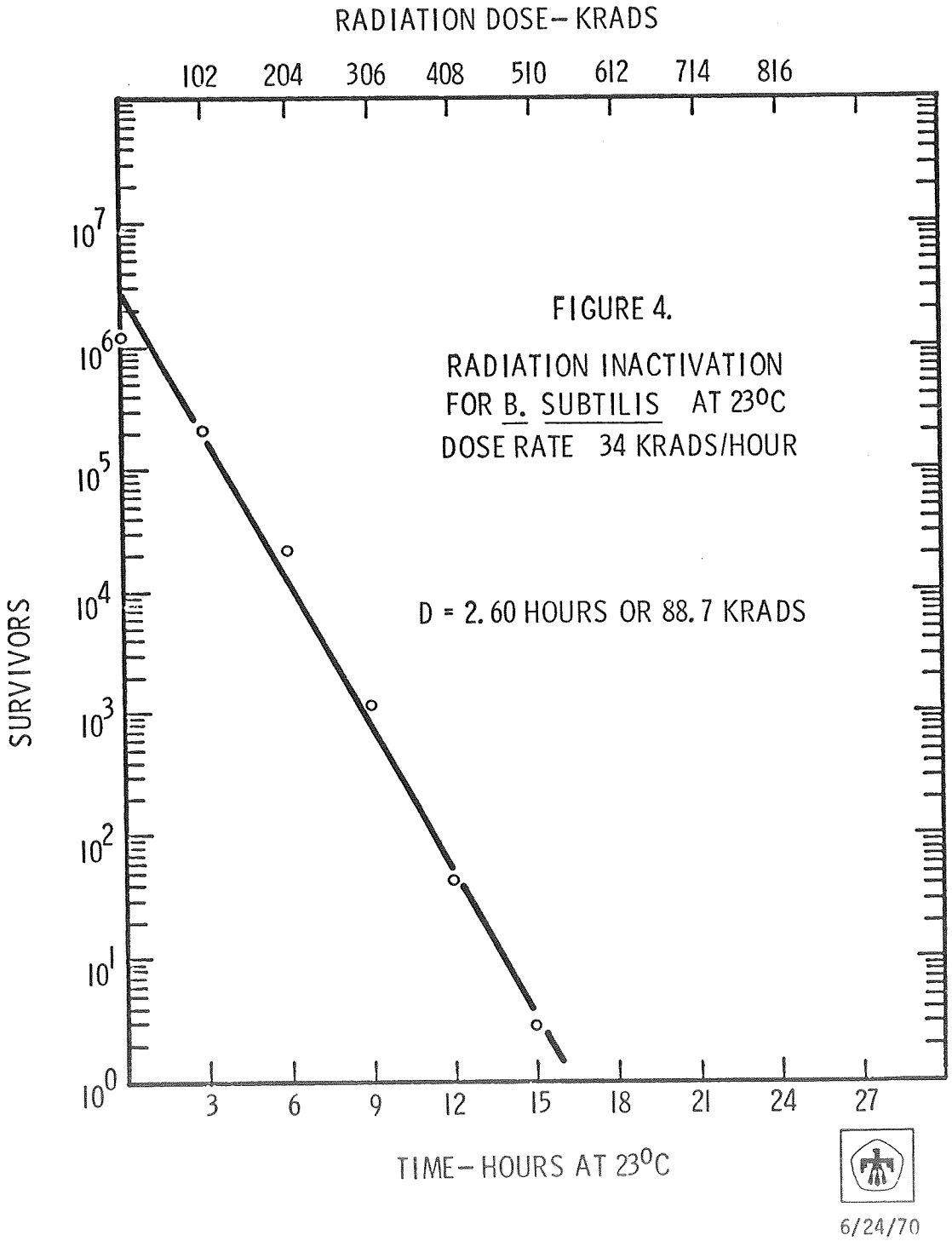

FIGURE 4.

RADIATION INACTIVATION
FOR B. SUBTILIS AT 23°C
DOSE RATE 34 KRADS/HOUR

D = 2.60 HOURS OR 88.7 KRADS

6/24/70

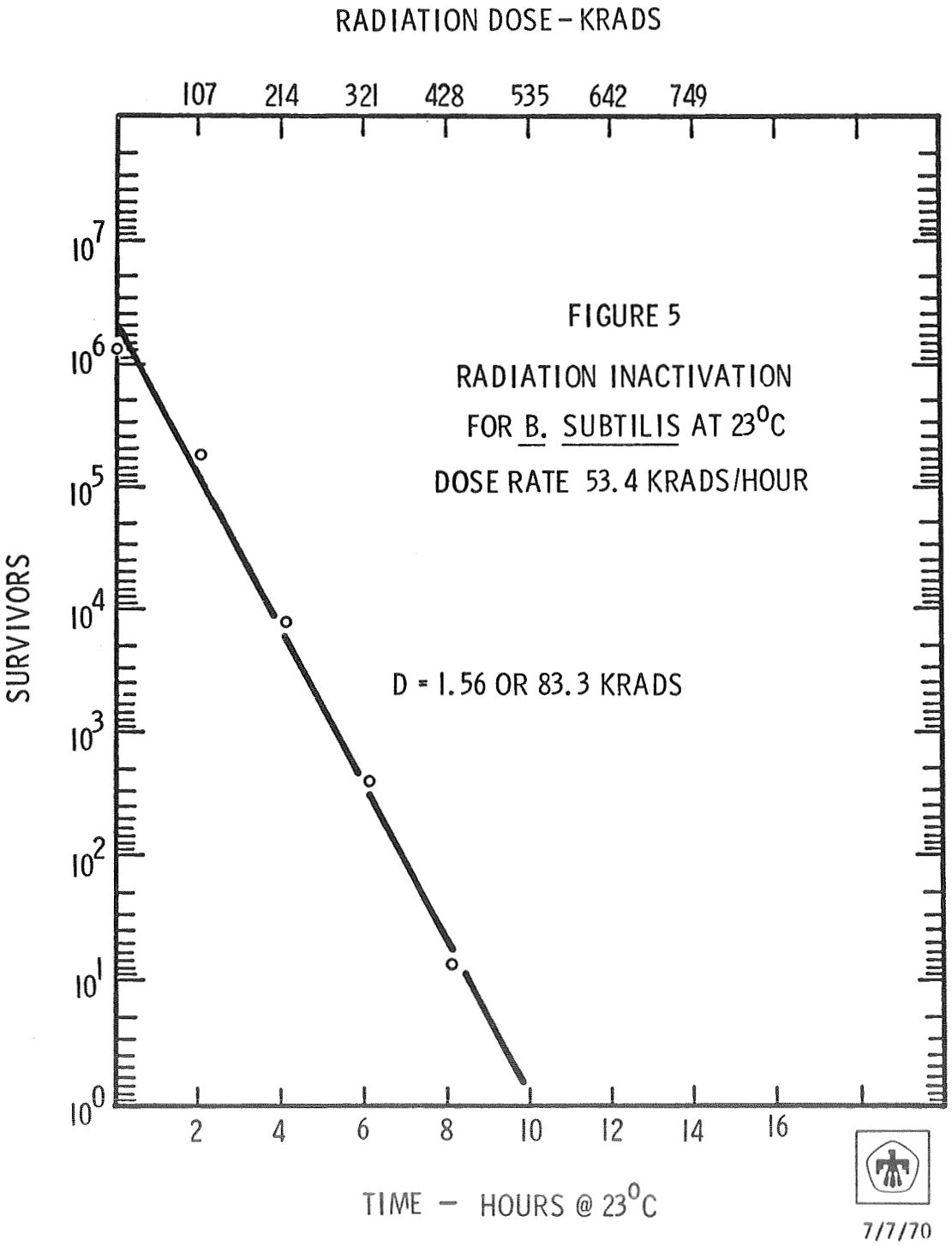
RADIATION DOSE - KRADS
107
214
321
428
535
642
749
SURVIVORS
10^7
10^6
10^5
10^4
10^3
10^2
10^1
10^0
2
4
6
8
10
12
14
16
TIME - HOURS @ 23°C
FIGURE 5
RADIATION INACTIVATION
FOR B. SUBTILIS AT 23°C
DOSE RATE 53.4 KRADS/HOUR
D = 1.56 OR 83.3 KRADS
7/7/70

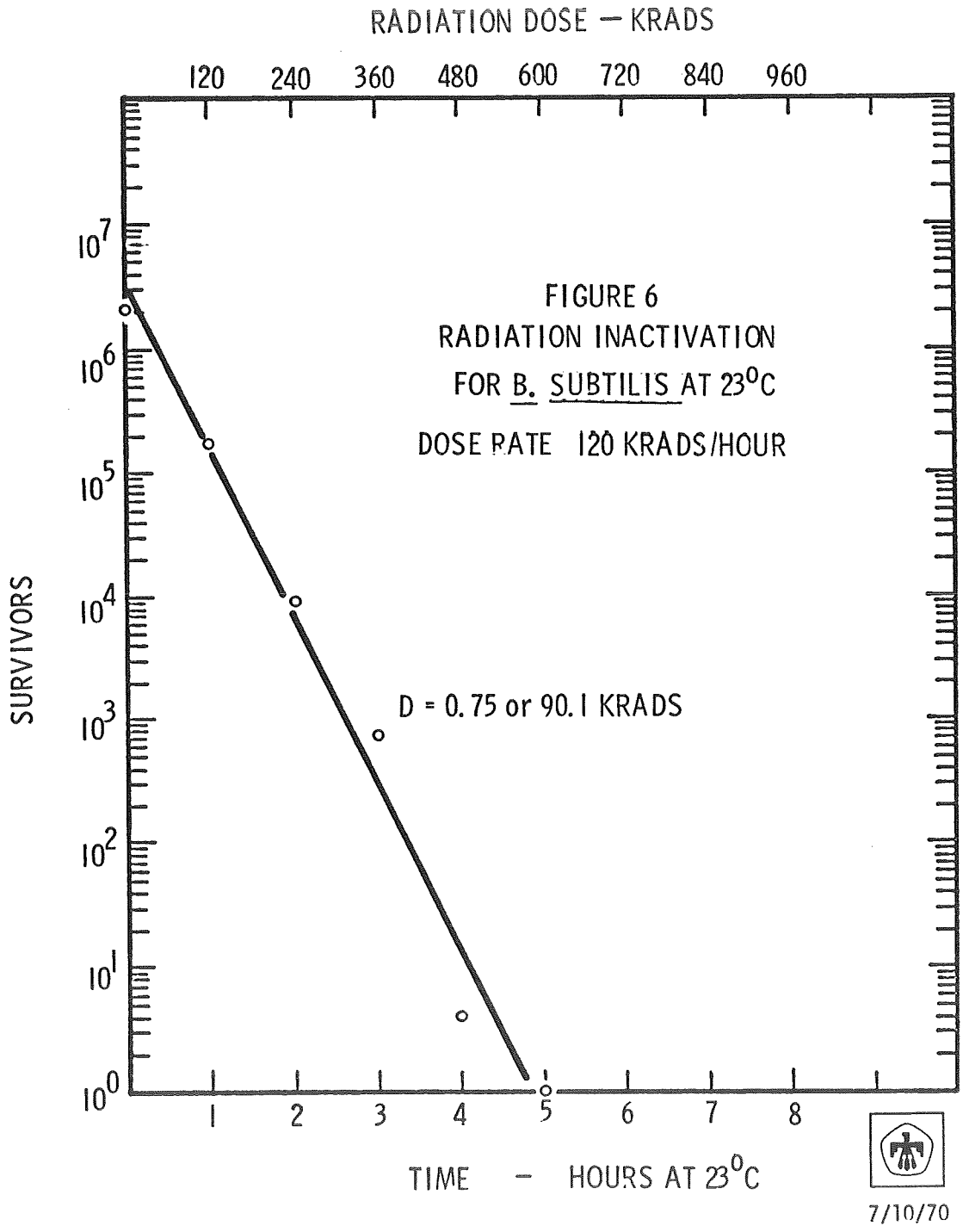

FIGURE 6
RADIATION INACTIVATION
FOR B. SUBTILIS AT 23°C
DOSE RATE 120 KRADS/HOUR

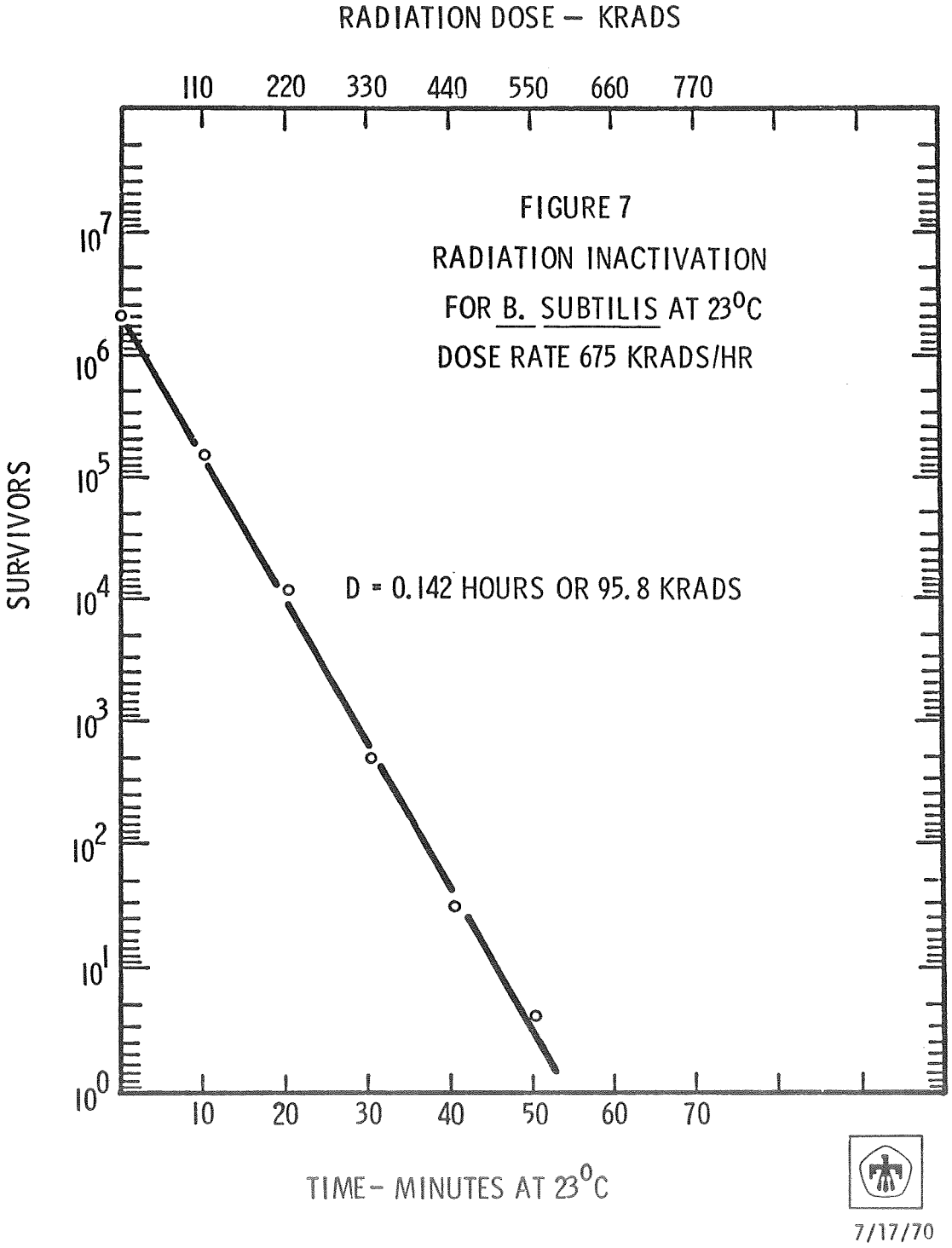
RADIATION DOSE – KRADS
110
220
330
440
550
660
770
FIGURE 7
RADIATION INACTIVATION
FOR B. SUBTILIS AT 23°C
DOSE RATE 675 KRADS/HR
D = 0.142 HOURS OR 95.8 KRADS
SURVIVORS
10^7
10^6
10^5
10^4
10^3
10^2
10^1
10^0
10
20
30
40
50
60
70
TIME – MINUTES AT 23°C
7/17/70

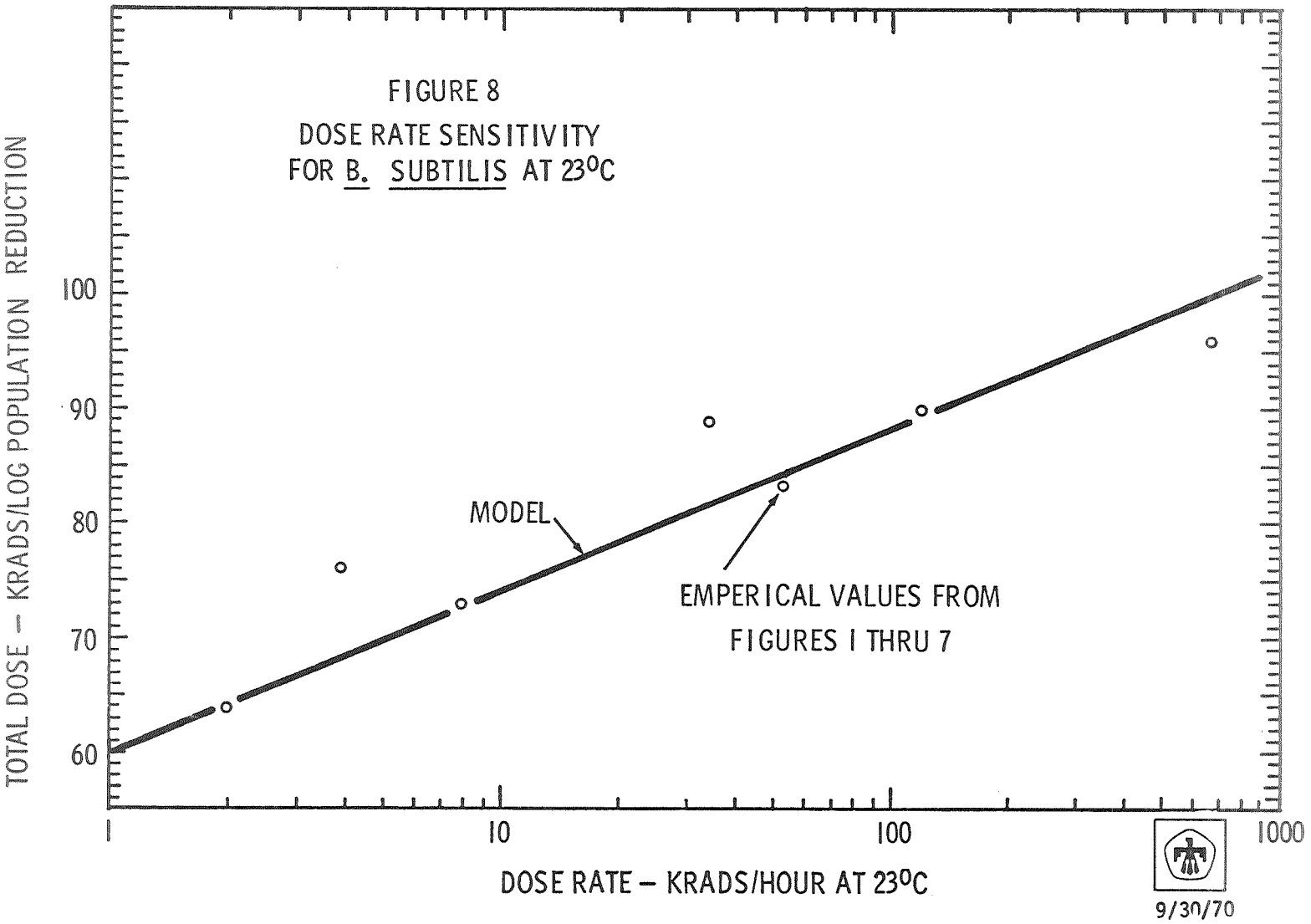
FIGURE 8
DOSE RATE SENSITIVITY
FOR B. SUBTILIS AT 23°C
TOTAL DOSE – KRADS/LOG POPULATION REDUCTION
100
90
80
70
60
MODEL
EMPERICAL VALUES FROM
FIGURES I THRU 7
1
10
100
1000
DOSE RATE – KRADS/HOUR AT 23°C
9/30/70

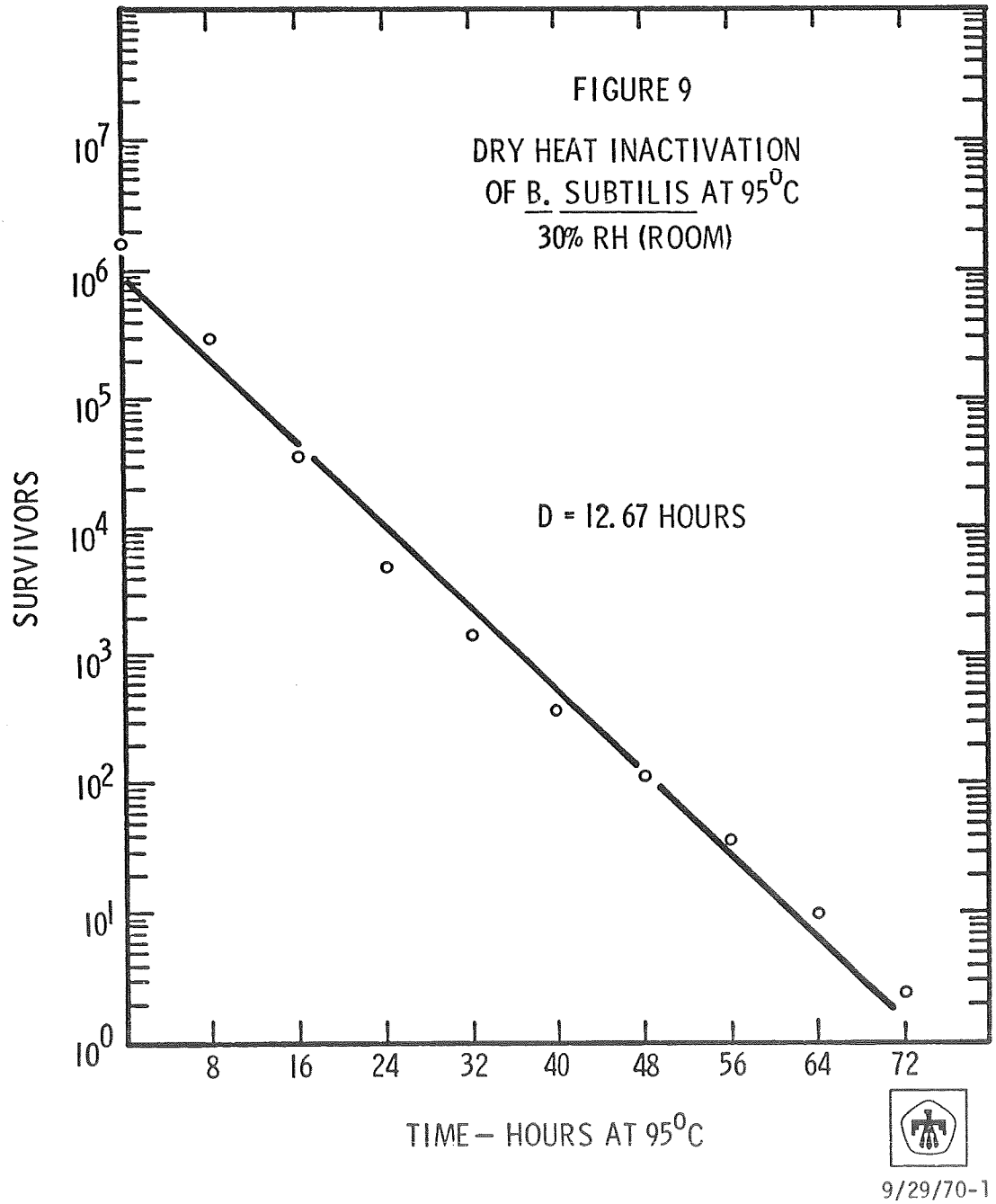
FIGURE 9
DRY HEAT INACTIVATION
OF B. SUBTILIS AT 95°C
30% RH (ROOM)
D = 12.67 HOURS
SURVIVORS
10^7
10^6
10^5
10^4
10^3
10^2
10^1
10^0
8
16
24
32
40
48
56
64
72
TIME – HOURS AT 95°C
9/29/70-1

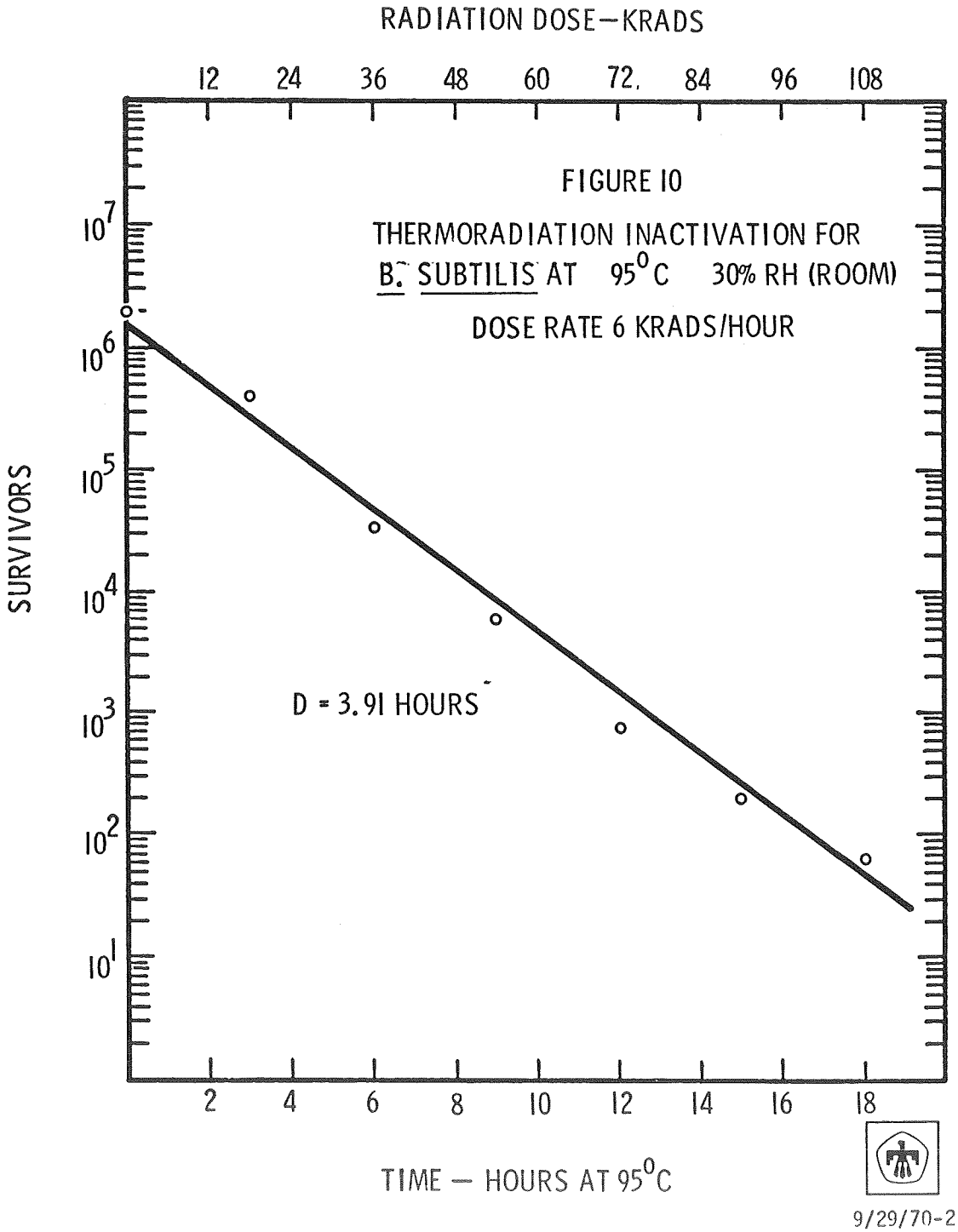
RADIATION DOSE—KRADS
12
24
36
48
60
72
84
96
108
FIGURE 10
THERMORADIATION INACTIVATION FOR
B. SUBTILIS AT 95°C 30% RH (ROOM)
DOSE RATE 6 KRADS/HOUR
SURVIVORS
10^7
10^6
10^5
10^4
10^3
10^2
10^1
D = 3.91 HOURS
2
4
6
8
10
12
14
16
18
TIME — HOURS AT 95°C
9/29/70-2

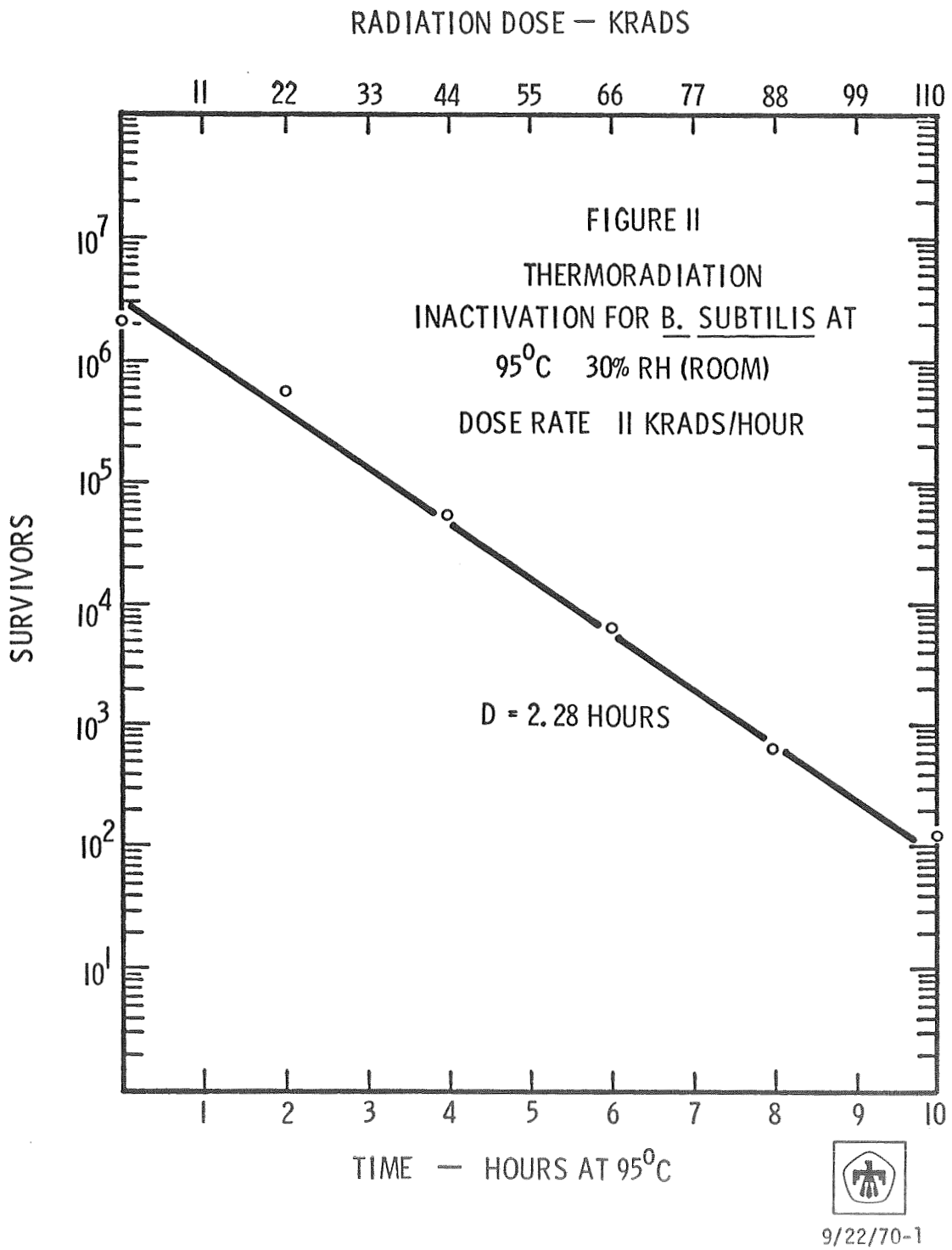
RADIATION DOSE — KRADS
11 22 33 44 55 66 77 88 99 110
SURVIVORS
10^7 10^6 10^5 10^4 10^3 10^2 10^1
FIGURE II
THERMORADIATION
INACTIVATION FOR B. SUBTILIS AT
95°C 30% RH (ROOM)
DOSE RATE 11 KRADS/HOUR
D = 2.28 HOURS
1 2 3 4 5 6 7 8 9 10
TIME — HOURS AT 95°C
9/22/70-1

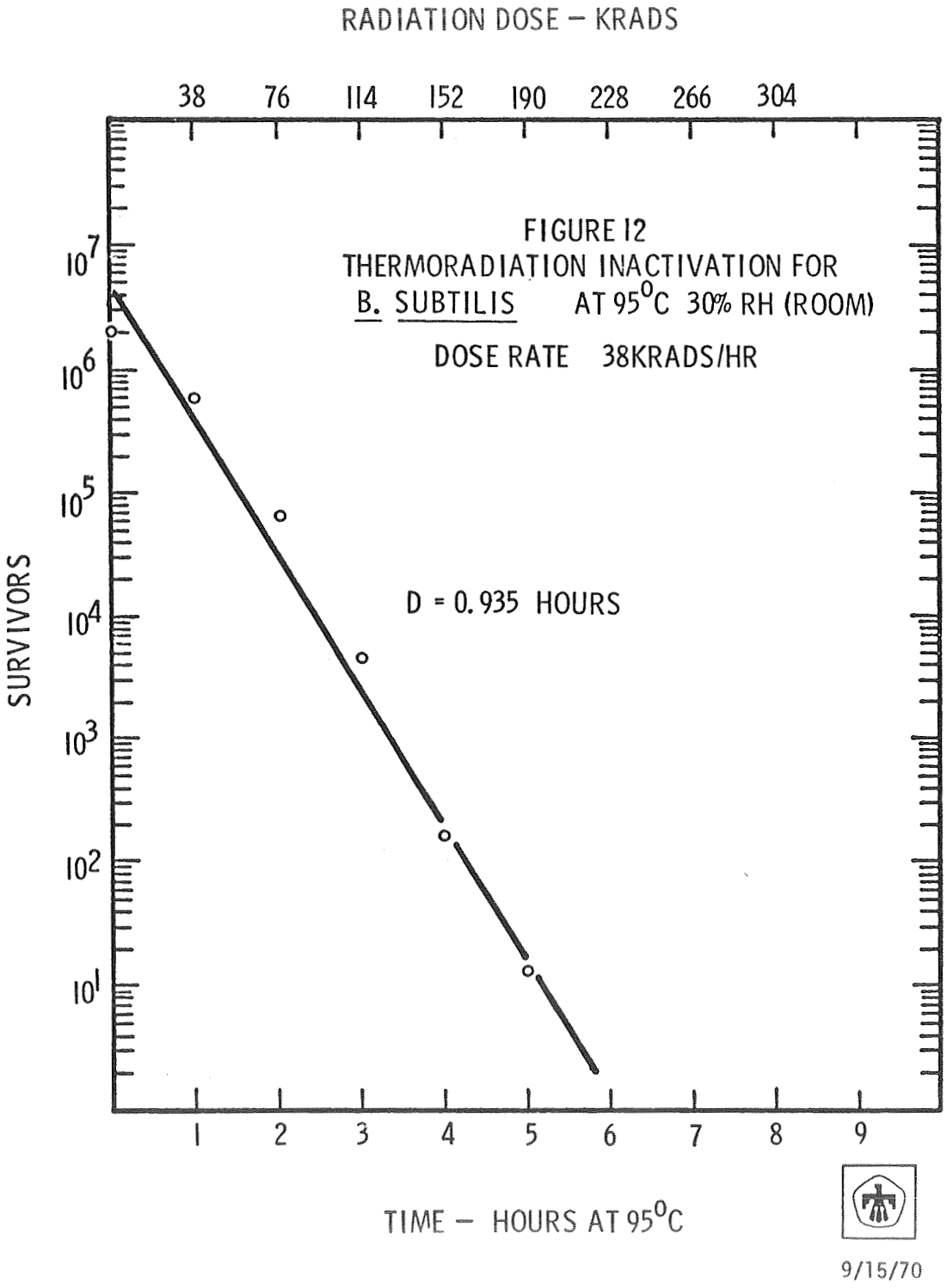
RADIATION DOSE – KRADS
38
76
114
152
190
228
266
304
FIGURE 12
THERMORADIATION INACTIVATION FOR
B. SUBTILIS AT 95°C 30% RH (ROOM)
DOSE RATE 38KRADS/HR
D = 0.935 HOURS
SURVIVORS
10^7
10^6
10^5
10^4
10^3
10^2
10^1
1
2
3
4
5
6
7
8
9
TIME – HOURS AT 95°C
9/15/70

FIGURE 13

THERMORADIATION
D VALUE VS. DOSE RATE
FOR B. SUBTILIS AT 95°C

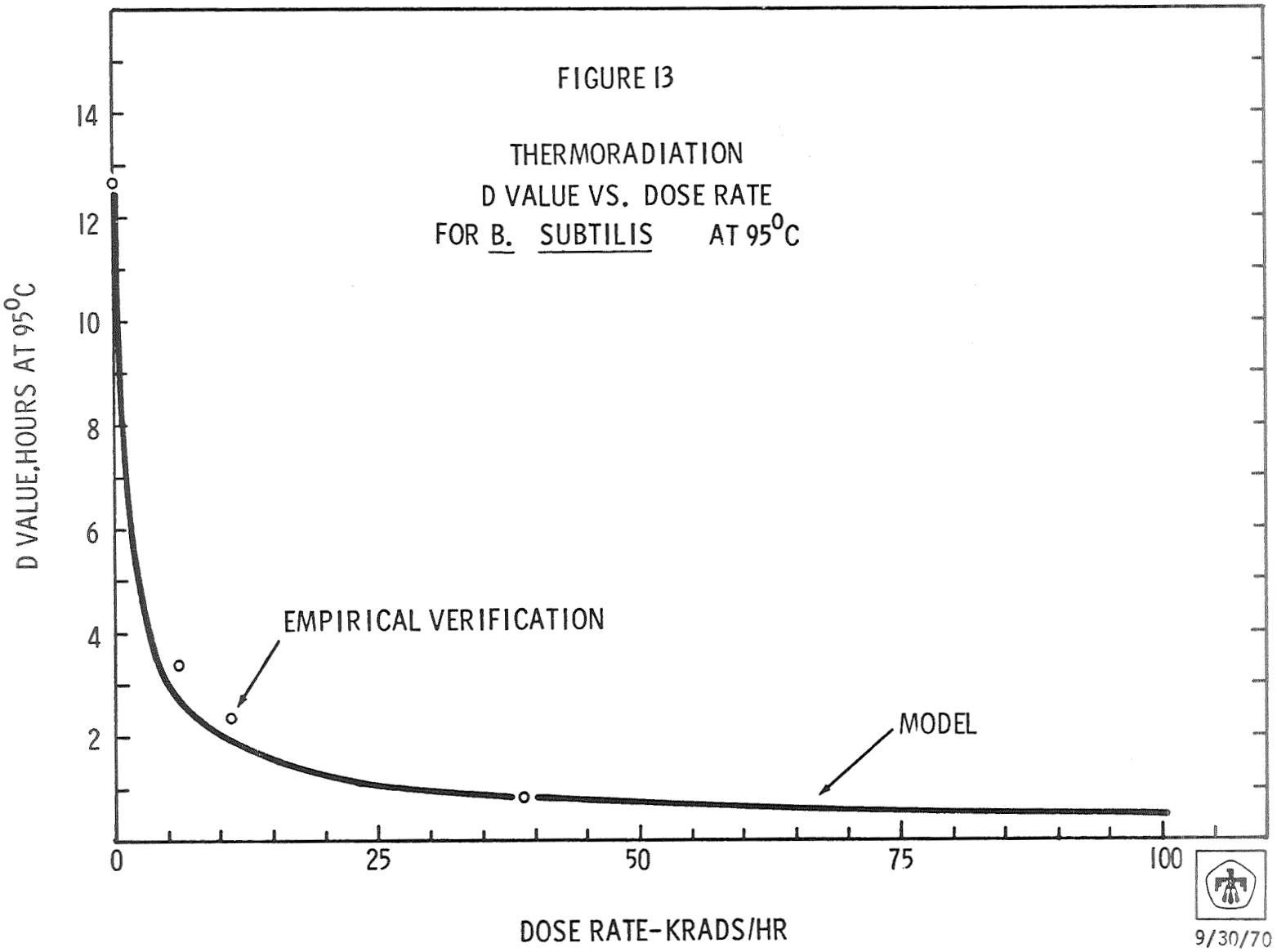

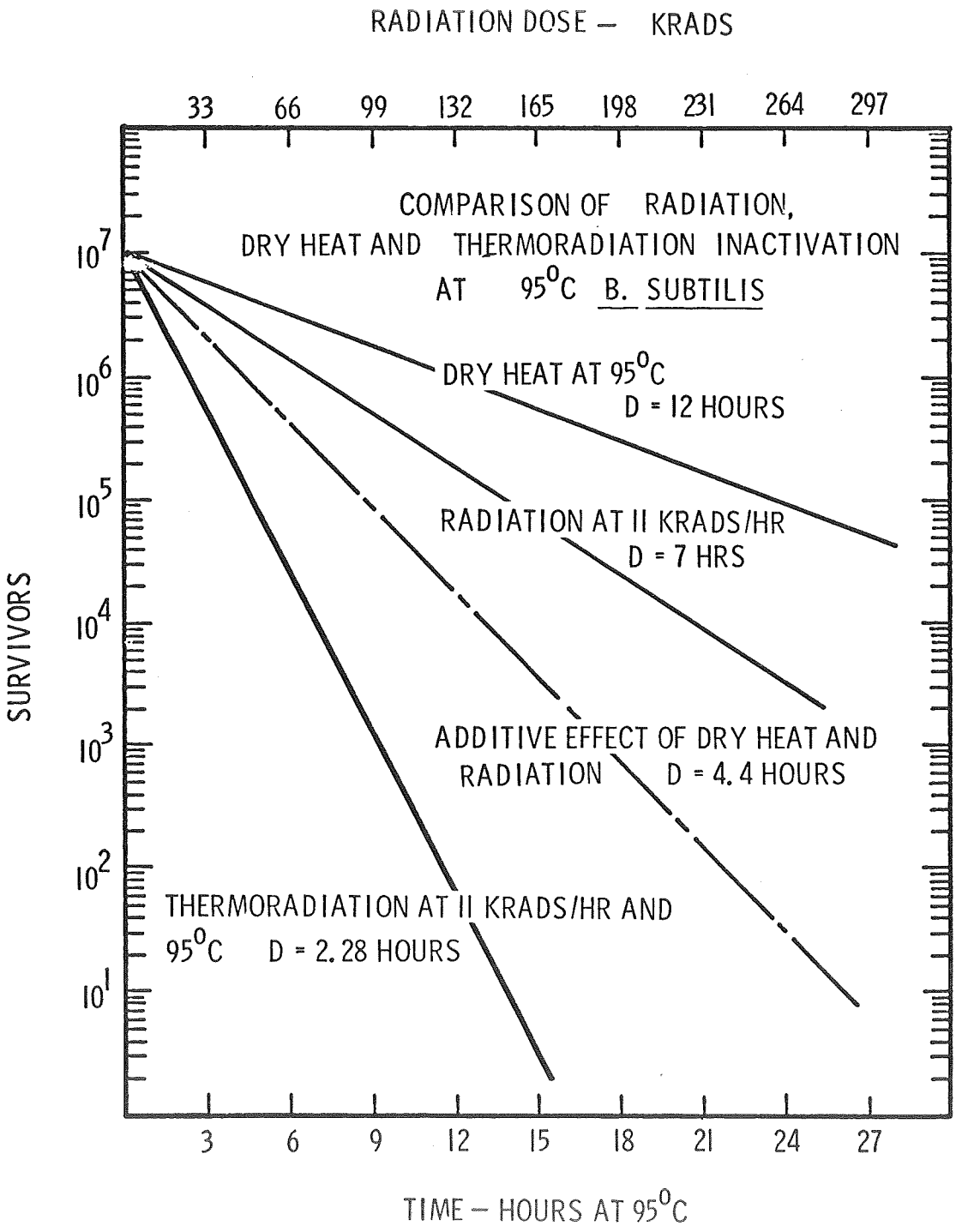
RADIATION DOSE — KRADS
33
66
99
132
165
198
231
264
297
COMPARISON OF RADIATION,
DRY HEAT AND THERMORADIATION INACTIVATION
AT 95°C B. SUBTILIS
DRY HEAT AT 95°C
D = 12 HOURS
RADIATION AT 11 KRADS/HR
D = 7 HRS
ADDITIVE EFFECT OF DRY HEAT AND
RADIATION D = 4.4 HOURS
THERMORADIATION AT 11 KRADS/HR AND
95°C D = 2.28 HOURS
SURVIVORS
10^7
10^6
10^5
10^4
10^3
10^2
10^1
3
6
9
12
15
18
21
24
27
TIME — HOURS AT 95°C

FIGURE 14

Modeling of Thermoradiation Synergism

A. Description. The objectives of this activity are to develop a physically based model representing bacterial spore inactivation in a composite environment of heat and ionizing radiation and to make this model available for analysis and for planning future work in this area. The models which are presented are of two basic interrelated types. The first model is the semi-empirical model which describes the bacterial spore inactivation rate as a function of radiation dose rate and temperature. The second model is a preliminary effort at completely generalizing a theoretical model describing the spore inactivation in the composite environment. The generalization of the previously reported theoretical model is being done with the constraints that it be able to fit the accumulated data and that it be in broad agreement with previous modeling efforts.

B. Progress.

1. Update of Parameter Values. The original parameter values for the empirical inactivation model

$$E[n(t)] = n(o)e^{-kt} \qquad (1)$$

$$k = \frac{KT}{h}\ e^{14.55}\ e^{-16890/T} + r_d^{\alpha/T}\ e^{\beta}\ e^{-\gamma/T} \qquad (2)$$

where T is temperature in degrees Kelvin and r_d is the gamma dose rate in kilorads per hour were based upon two ambient temperature data points obtained over 1 1/2 years ago. This

quarter a more complete set of ambient temperature radiation inactivation data has been obtained and this has allowed a possible refinement of the parameter values. This determination of new parameter values has been carried out in two different ways.

First, to demonstrate the validity of the model as a useful predictive tool, the parameters α, β, and γ were calculated using experimentally determined reaction rate constants at 25°C and radiation dose rates of 8 and 32 kilorads per hour and at 105°C and 22 kilorads per hour. These three data points provided the values α = 276 degrees Kelvin, β = 4.75 and γ = 2403 degrees Kelvin. An indication of how well these parameter values can provide accurate inactivation prediction is shown in Figure 1 where other data points are compared with the model generated predictions.

The second method for parameter determination centered about determining an "optimal" set of parameter values. The sense in which this was done was to (1) define α as a running index, (2) calculate β and γ for every possible combination of 17 representative data points taken two at a time, (3) find the mean value of β and γ, and (4) select the optimal value of α and its corresponding mean values of β and γ on the basis of finding

$$\min_{\alpha,\beta,\gamma} \sum_{i=1}^{17} \left| k_{Mi} - k_{Di} \right| \qquad (3)$$

where k_{Mi} is the model generated reaction rate constant and k_{Di} is the experimental value for the same temperature and dose rate. The solution to equation (3) provided α = 260.0

degrees Kelvin, β = 5.01 and γ 2439 degrees Kelvin. These parameters are in close agreement with those based only on three data points, and the value of equation (3) for the first set of parameters is only 0.1 greater than that for the second set.

The most obvious observation concerning these new parameter determinations as compared to the original set is that α has increased from 218°K to somewhere in the range 260 - 276°K. This indicates that the nonlinear radiation dose rate dependence terminates in the range -13°C to 3°C rather than at approximately -55°C as originally observed.

2. Thermoradiation Temperature Requirements. If thermoradiation were employed as a sterilization mechanism, then there would be some upper limit D imposed on the total gamma dose which could be used without risking radiation damage to the more sensitive spacecraft components. If equation (1) is assumed as the form of the inactivation curve of the bacteria on the spacecraft and if the integration of heat-up and cool down times are ignored for simplicity, then at the end of the sterilization cycle of t_s hours and p logs of population reduction the condition will be

$$n(o)e^{-kt_s} = n(o) \cdot 10^{-p} \qquad (4)$$

or

$$kt_s = p\ln 10 = 2.303p. \qquad (5)$$

Also, if the maximum total dose D_s is utilized, then

$$r_d t_s = D_s. \qquad (6)$$

Equations (5) and (6) may be used to calculate the temperature and time required to provide a p log population reduction with a maximum total dose D for a family of radiation dose rates. The solution of equation (5) for the temperature T is most easily done numerically. These calculations are illustrated in Figure 2 for an 8 log population reduction. In Figure 2 the temperature required for the specified population reduction is plotted as a function of the total radiation dose used for the selected family of radiation dose rates. Also plotted is a family of isotime lines or, in other words, a family of loci for which the sterilization time t_s is a constant. As an example, consider the locus for t equal 5 hours. The temperatures and radiation doses required for the 8 log population reduction are 116.37°C and 50 kilorads, 113.34°C and 100 kilorads, 109.93°C and 150 kilorads, 105.71°C and 200 kilorads, and 100.13°C and 250 kilorads for dose rates of 10, 20, 30, 40 and 50 kilorads per hour respectively. Figure 2 also illustrates that the minimization of the sterilization temperature is accomplished by using the lowest possible dose rate which will not exceed some upper bound on sterilization time for any specified total dose. Again, as an example, for a maximum dose of 150 kilorads and a maximum time t_s = 5 hours, the lowest sterilization temperature is 109.93°C at a dose rate of 30 kilorads per hour. This may be compared with the temperature requirement for dry heat alone for the same 8 log population reduction

within the same 5 hour period. This temperature would be 120°C for the stock of B. subtilis which is being modeled.

3. Further Theoretical Modeling. The theoretical kinetic model which was described in SC-RR-70-203 and in QR-16 represents the inactivation of a bacterial spore's critical substrate A by a free radical population R at a rate k_1 and the simultaneous inactivation of the same substrate by heat at a rate k_T. These inactivations are schematically represented as

$$A \xrightarrow{k_T} D \qquad (7)$$

and

$$A + R \xrightarrow{k_1} X \qquad (8)$$

where D and X represent inactivated states of the critical substrate A and infer death of the spore. In the first development of this kinetic model the free radical population was explicitly defined by the equation

$$R(t) = C_R\,(r_d,T) \cdot \left(1 - e^{-k_3 t}\right) + C_2\,(r_d,T) \cdot e^{-k_2 t} \qquad (9)$$

where $C_R(r_d,T)$ represents an equilibrium concentration of free radicals and $C_2(r_d,T)$ represents a concentration of radicals resulting from any preirradiation treatment. Some effort has been devoted this quarter to the task of defining R(t) by a rational kinetic reaction rather than by the explicit definition

of equation (9).

The most promising results in this investigation have come from defining a very generalized substrate S which is probably composed of a variety of materials that provide the free radicals R when irradiated with gamma photons. This generation of R may be more completely described by the reversible reaction

$$S \underset{k_4}{\overset{k_R}{\rightleftharpoons}} R + Q \qquad (10)$$

where Q is also a free radical species which does not necessarily affect the critical substrate A. The reaction rate parameter k_R is a function of the radiation dose rate and describes the rate of production of R, and the parameter k_4 is a function of temperature and describes the rate of recombination of the two radical species. The generalized substrate S is assumed to be dependent upon the conditions under which the spores are treated with thermoradiation - such as the embedding matrix, the relative humidity, the oxygen partial pressure, etc.

The nonlinear differential equations which describe the inactivation process are

$$dA/dt = - k_T A - k_1 RA \qquad (11)$$

and

$$dR/dt = k_R S - k_4 QR - k_1 AR \qquad (12)$$

Two cases are now considered for the definition of S and Q. For the first possible situation, assume that the supply of S is relatively constant and appears as a self-regulating system. This could be the case if S represented a water vapor or an oxygen dependent substrate and if the spores were exposed in an open system. For this case

$$dS/dt = 0 \tag{13}$$

and

$$dQ/dt = k_R S - k_2 QR \tag{14}$$

where the constant representing S is an added parameter. The solution of this complete set of equations provides results in good agreement with the experimental results for open systems. With S a constant, R builds up to some equilibrium concentration very rapidly and changes only slightly for the remainder of the period of interest. This is consistent with the concept expressed in equation (9) where $C_R(r_d,T)$ is the equilibrium concentration and k_3 is the rate at which this concentration is approached.

For the second possible situation of interest, S is a substrate which has some initial value but is depleted and not replenished when the free radicals are produced. This could be the case when the spores are embedded in a nonporous matrix such as methyl-methacrylate or in a closed air-tight container and are subsequently treated with thermoradiation. Here the applicable differential equation is

$$dS/dt = - k_R S + k_4 QR \qquad (15)$$

with

$$Q = S_o - S \qquad (16)$$

where S_o is the initial concentration of S. The general solution of the complete set of equations for this case allows R to build up rapidly at first but then decrease to a low concentration as the concentration of S is depleted. This can explain the rapid initial inactivation followed by a much slower subsequent rate for spores embedded in methacrylate.

In either case, describing R in this manner provides an explanation for the inactivation rate or D value for spores being dependent upon the initial loading as reported in SC-RR-69-857. As previously pointed out, both equations (11) and (12) are nonlinear. Since they are nonlinear, their solutions will inherently depend upon the initial values of both A and R. More specifically, the build up and subsequent behavior of the free radical concentration R is dependent on the initial concentration of A as shown in equation (12), and the rate of decrease in A is very dependent upon the concentration of R. Therefore, changing the initial loading affects the radical concentration and the rate of inactivation of A in a coupled, nonlinear manner.

The formulation of equation (12) also provides a rational explanation for the reaction rate parameter k of equation (2) being a

nonlinear temperature dependent function of the radiation dose rate. Once again the rate of inactivation of A at any temperature is dependent on the concentration of R; however, the concentration of R is both dependent upon the dose rate and upon the temperature during irradiation. This nonlinear coupling of the dose rate and temperature effects may provide the empirical description in equation (2).

Efforts are now under way to determine the description of the rate parameters k_1, k_2, and k_R which will be consistent with the information obtained from the formulations of equations (2) and (9) and with the form of the experimental results. The solutions for the sets of equations are being determined numerically using a fourth order Runge-Kutta routine with a step size of .01 to .001 hours. The gross nonlinearity of the set of equations promises to provide some interpretations of the anomalous experimental results obtained at a very low dose rate and a temperature of 105°C.

4. Mathematical Generalization of Synergistic Inactivation. A simple mathematical explanation of "synergistic inactivation" in heated microbial inactivation processes has been developed. This explanation compares the degree of inactivation of a microbial population in a combined environment of heat and any chemically acting antimicrobial agent with the sum of the inactivations of heat and the antimicrobial agent acting alone for equal periods of time. The basis for the observed "synergism" is shown to be simply the temperature dependence of the chemically active agent.

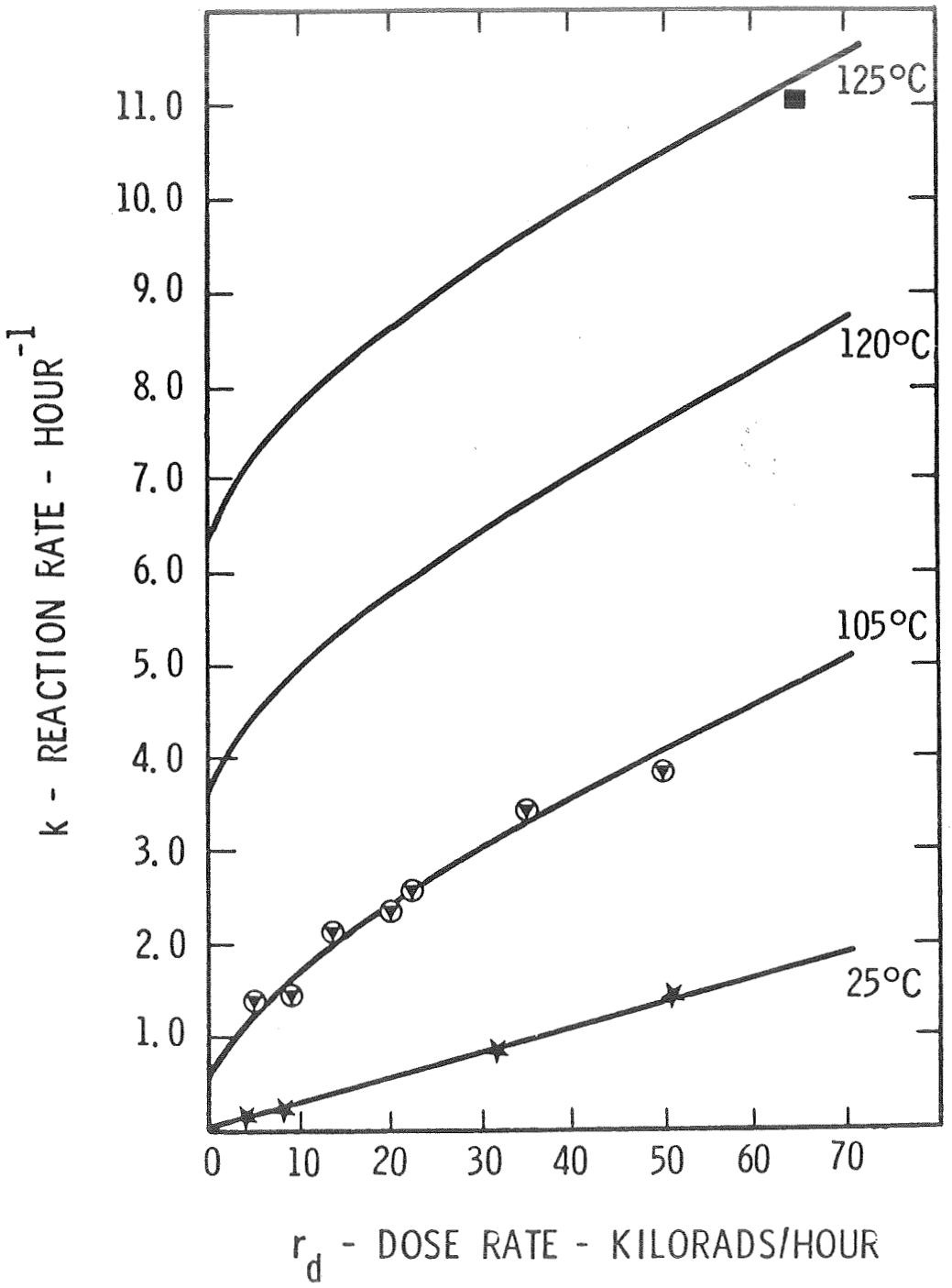

FIGURE 1. A Comparison of Experimental Results With Model Predictions of the Inactivation Rate of Bacillus subtilis var. niger spores.

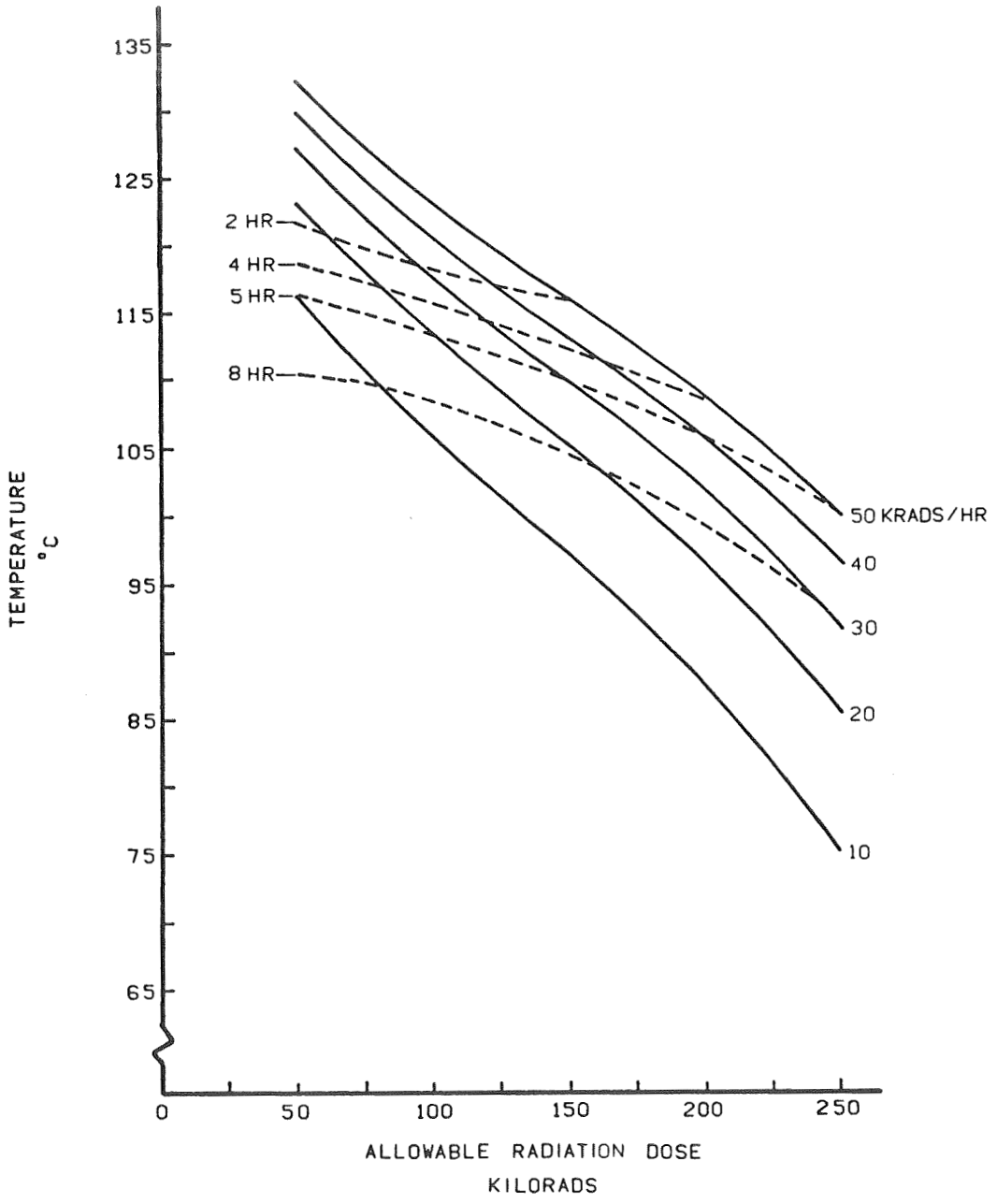

FIGURE 2. Temperature Requirement as a Function of Allowable Radiation Dose for an Eight Log Reduction in a Population of Bacillus subtilis var. niger spores. Dashed Lines are Lines of Isotime.

Thermoradiation Inactivation In Open and Closed Systems

A. Description. The objective of these experiments is to develop a practical experimental protocol which can be used to study the parameters affecting the rate of inactivation of bacterial spores by thermoradiation in a closed system. In the course of this study, it is hoped that at least a partial understanding of the decreased rate of inactivation in matrices such as methylmethacrylate, gelatin, epoxy, etc., will be obtained and that practical models of closed systems can be developed.

B. Progress. Last quarter, the feasibility of using simple closed aluminum systems to approximate the behavior of methylmethacrylate systems was demonstrated. This was done using aluminum ampoules constructed by drilling 3/8-inch diameter holes, 3/4-long into 1-inch sections of 1/2-inch aluminum bar stock. The mouth of each ampoule was threaded for a 1/4-inch long, 3/8-inch x 24 socket head screw which was equipped with a tightly fitting 1/4-inch rubber "O" ring.

Subsequently, the aluminum ampoules were loaded by placing 0.5 ml of 2×10^7 per ml ethanol suspension of Bacillus subtilis var. niger spores into the cavity and evaporating the ethanol into a partial vacuum (25 in. Hg) for approximately 16 hours over a desiccant. For experimentation, the ampoules were arranged in groups of six in small aluminum racks and placed in the composite heat-radiation environment with three of the six ampoules sealed and three open.

After exposure, the spores were removed from the ampoules by depositing each ampoule (open end down) in a flat bottomed cylindrical glass bottle filled with 25 ml of cold 1-percent peptone water and sonicating for two minutes. Data taken at 20 krads/hour and 120°C and 105°C are shown in Figures 1 and 2. This past quarter, data were obtained additionally at 112°C and 20 krads/hour. This is shown in Figure 3. Moisture and pressure values for these systems is shown in Table 1.

TABLE 1

System	Approx. RH (@ temp)	Approx. Pressure (@ temp,atm.)
120°C Open	0.28%	0.827
Closed	0.38%	1.104
112°C Open	0.35%	0.827
Closed	0.48%	1.082
105°C Open	0.45%	0.827
Closed	0.59%	1.062

The RH values in Table 1 include only atmospheric moisture. These values lie approximately in a range where previous experimentation (cf. QR 14) indicates thermoradiation inactivation is insensitive to moisture. On the other hand, should additional moisture from oxide layers be present, this may not be true.

In an attempt to determine whether moisture trapped in oxide layers in the aluminum ampoules might be a partial cause of the phenomenon seen in Figures 1, 2 and 3, a closed system experiment was run in glass ampoules. The large end of Pasteur pipettes were

flame sealed and the pipettes were sterilized and loaded with 0.5 ml of the previous 2 x 10^7 ethanol spore suspension using a 1 ml syringe. These pipettes were dried rapidly (20 sec.) at 100°C and under 25 in. Hg vacuum and then allowed to stand in a vacuum for 16 hours over a desiccant. Next they were allowed to stand 24 hours at ambient pressure and an RH of approximately 20%. The small ends were then flame sealed, and the ampoules were exposed to a thermoradiation environment of 120°C and 20 krads/hour. To recover the spores the small end of the pipette was cut off and 1 ml of sterile 1-percent peptone water was added. The pipette was then sonicated for two minutes. Data for this closed glass system were somewhat like that for the closed aluminum system under the same conditions - but were sufficiently erratic to leave doubt about possible moisture effects. Thus, this approach did not rule out moisture as a partial cause of the differences observed between open and closed systems.

Because of the indeterminancy of the above approach, it was simply assumed that pressure is the major causative factor in the difference in inactivation rates between open and closed systems in thermoradiative environments, and then the reasonableness of this assumption was investigated.

Using the model previously developed for thermoradiation (cf. QR's 15 and 16) the population was assumed to behave according to the equation

$$E[n(t)] = n(o)\, e^{-kt}$$

where n(t) is the surviving population at time t, E denotes

mathematical expectation and $k = k_T + k_S$ is the chemical inactivation rate of some spore substance A by the reactions

$$A \xrightarrow{k_T} B, \qquad A + R \xrightarrow{k_1} C.$$

where R is the free radical concentration.

Combining this previous work on the form of k in thermoradiative environments with the work incorporating pressure into spore inactivation (cf. QR 15 and 16) yields k in the form

$$k = \frac{KT}{h} e^{-(\Delta H_o^{\neq} - T\Delta S_o^{\neq} + p\Delta V^{\neq})/RT} + r_d^{\alpha/T} e^{-(\Delta \mathcal{H}_o^{\neq} - T\Delta \mathcal{S}_o^{\neq} + p\Delta \mathcal{U}^{\neq})/RT}$$

where K is Boltzman's constant, h is Planck's constant, R is the gas constant, α is an empirically determined parameter related to the steady state free radical concentration, $\Delta H_o^{\neq}$, $\Delta \mathcal{H}_o^{\neq}$, and $\Delta S_o^{\neq}$, $\Delta \mathcal{S}_o^{\neq}$ are the zero pressure activation enthalpies and zero pressure activation entropies respectively, $\Delta V^{\neq}$ and $\Delta \mathcal{U}^{\neq}$ are the activation volumes of the reaction types A$\rightarrow$B and A + R$\rightarrow$C respectively, and p is the absolute pressure at which these reactions take place. The temperature, T, is in degrees Kelvin, and r_d is the radiation dose rate in kilorads per hour.

At ambient pressure p_o and a dose rate r_d, one gets for two temperatures T_1 and T_2

$$k_1 = e^{\Delta S_o^{\neq}/R} \frac{KT_1}{h} (x)^{1/T_1} + r_d^{\alpha/T_1} (y)^{1/T_1} e^{\Delta \mathcal{S}_o^{\neq}/R}$$

and

$$k_2 = e^{\Delta S_o^{\neq}/R} \frac{KT_2}{h} (x)^{1/T_2} + r_d^{\alpha/T_2} (y)^{1/T_2} e^{\Delta \mathcal{S}_o^{\neq}/R}$$

where

$$x = e^{-(\Delta H_o^{\neq}/R + p_o \Delta V^{\neq}/R^1)}$$

and

$$y = e^{-(\Delta \mathcal{H}_o^{\neq}/R + p_o \Delta \mathcal{U}^{\neq}/R^1)}$$

where R^1 is the gas constant in c.c. · ATM./Deg. · mole.

Since the data from the open systems agrees with data obtained previously from aluminum foil systems (cf. QR 15), the values of $\Delta S_o^{\neq}$, $\mathcal{S}\Delta_o^{\neq}$, and α are already known. Under these circumstances, we may regard

$$a = \frac{K}{h} e^{\Delta S_o^{\neq}/R}$$

and

$$b = e^{\Delta \mathcal{S}_o^{\neq}/R}$$

as known, and the above two equations take the form

$$\left.\begin{aligned} k_1 &= aT_1\,(x)^{1/T_1} + br_d^{\alpha/T_1}\,(y)^{1/T_1} \\ k_2 &= aT_2\,(x)^{1/T_2} + br_d^{\alpha/T_2}\,(y)^{1/T_2}. \end{aligned}\right\} \quad *$$

Here k_1 and k_2 are obtained from the survival data ($k = \mathrm{Log}_e 10/D$, where D is the D-value) and T_1, T_2, r_d and α are known. Thus, equations * represent two equations in two unknowns and, in this case, must be solved numerically for x and y for each of the three pairs of temperatures: (105°C, 112°C), (105°C, 120°C), and (112°C, 120°C). In each case the values were essentially the same, so that the average values x = EXP(-17044) and y = EXP(-2730) were used.

Next, we observe that for pressures p, other than ambient (p_o),

$$k_p = e^{\Delta S_o^{\neq}/R}\,\frac{KT}{h}\left[x \cdot e^{-(p-p_o)\Delta V^{\neq}/R^1}\right]^{1/T}$$

$$+\, e^{\Delta g_o^{\neq}/R}\, r_d^{\alpha/T}\left[y \cdot e^{-(p-p_o)\Delta \upsilon^{\neq}/R^1}\right]^{1/T}$$

where x and y are known from above, leaving only $\Delta V^{\neq}$ and $\Delta \upsilon^{\neq}$ as unknowns (k_p being again obtained from the survivor data). Hence, data from any elevated temperatures (and hence pressures different from ambient in the closed systems) yields two equations in which only $\Delta V^{\neq}$ and $\Delta \upsilon^{\neq}$ appear as unknowns. These unknowns may be determined numerically and the results of doing this are shown in Table 2.

TABLE 2

	(105°C,112°C)	(105°C,120°C)	(112°C,120°C)	Avg.
$\Delta V^{\neq}$ liters/mole	58	139	206	134
$\Delta U^{\neq}$ liters/mole	182	152	104	146

Since the values of $\Delta V^{\neq}$ and $\Delta U^{\neq}$ are extremely sensitive to changes in inactivation rate k, the variability found in Table 2 is easily accounted for by natural variability in survivor data.

Generally, however, this demonstrates that inactivation volumes in the ranges 58 to 206 liters/mole are adequate to explain the difference in survivor curves in open and closed systems in thermo-radiation environments. To determine whether the assumption that pressure is a major causative factor in the slow rate of inactivation in closed systems is reasonable, one may ask whether values of $\Delta V^{\neq}$ and $\Delta U^{\neq}$ in this range are reasonable values physically. One means of doing this is to ask what percentage volume change of various spore constituents would activation volumes of this magnitude represent, and whether such a percent change is compatible with those known to occur in small molecules. To make this comparison, one must first know the molar volumes of spore constituents that might be regarded as likely candidates for the substrate, A, being degraded. The most predominant member of the substrate A is probably the DNA molecule which has a molar volume of approximately 1.375×10^6

liters/mole (Watson, 1955, p. 85 and Katz & Schachman, 1955). The average value of $\Delta V^{\neq}$ listed in Table 2 is 134 liters/mole, and this represents a .0097% change in the molar volume of the DNA. Similarly the average value of $\Delta \upsilon^{\neq}$ represents a .0106% change in the DNA molar volume. Both of these percentages are consistent with percentage changes known to take place for smaller molecules. On this basis the values which were determined for $\Delta V^{\neq}$ and $\Delta \upsilon^{\neq}$ could be termed as being "feasible."

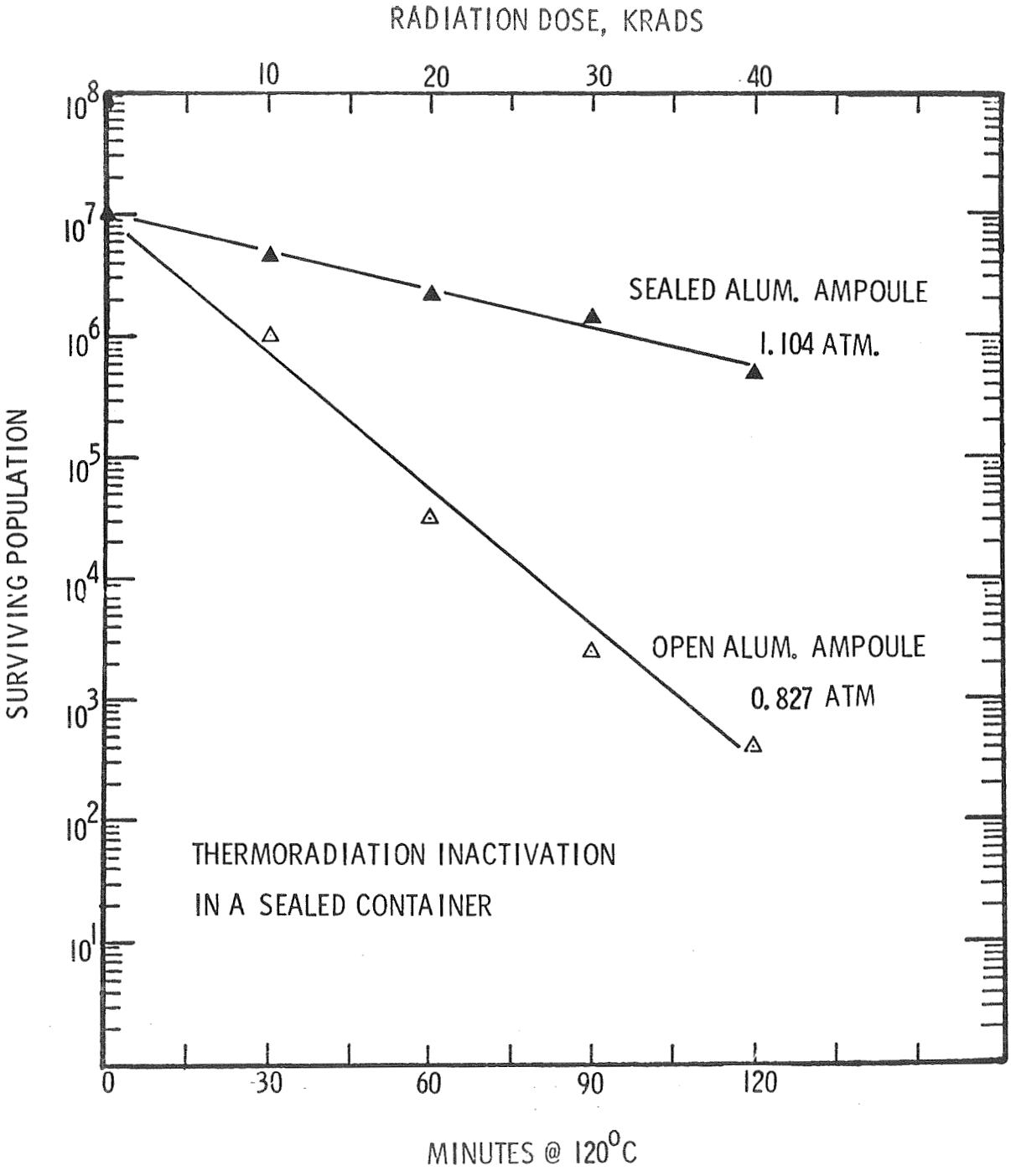
RADIATION DOSE, KRADS
10
20
30
40
10^8
10^7
10^6
10^5
10^4
10^3
10^2
10^1
SURVIVING POPULATION
SEALED ALUM. AMPOULE
1.104 ATM.
OPEN ALUM. AMPOULE
0.827 ATM
THERMORADIATION INACTIVATION
IN A SEALED CONTAINER
0
30
60
90
120
MINUTES @ 120°C

FIGURE 1

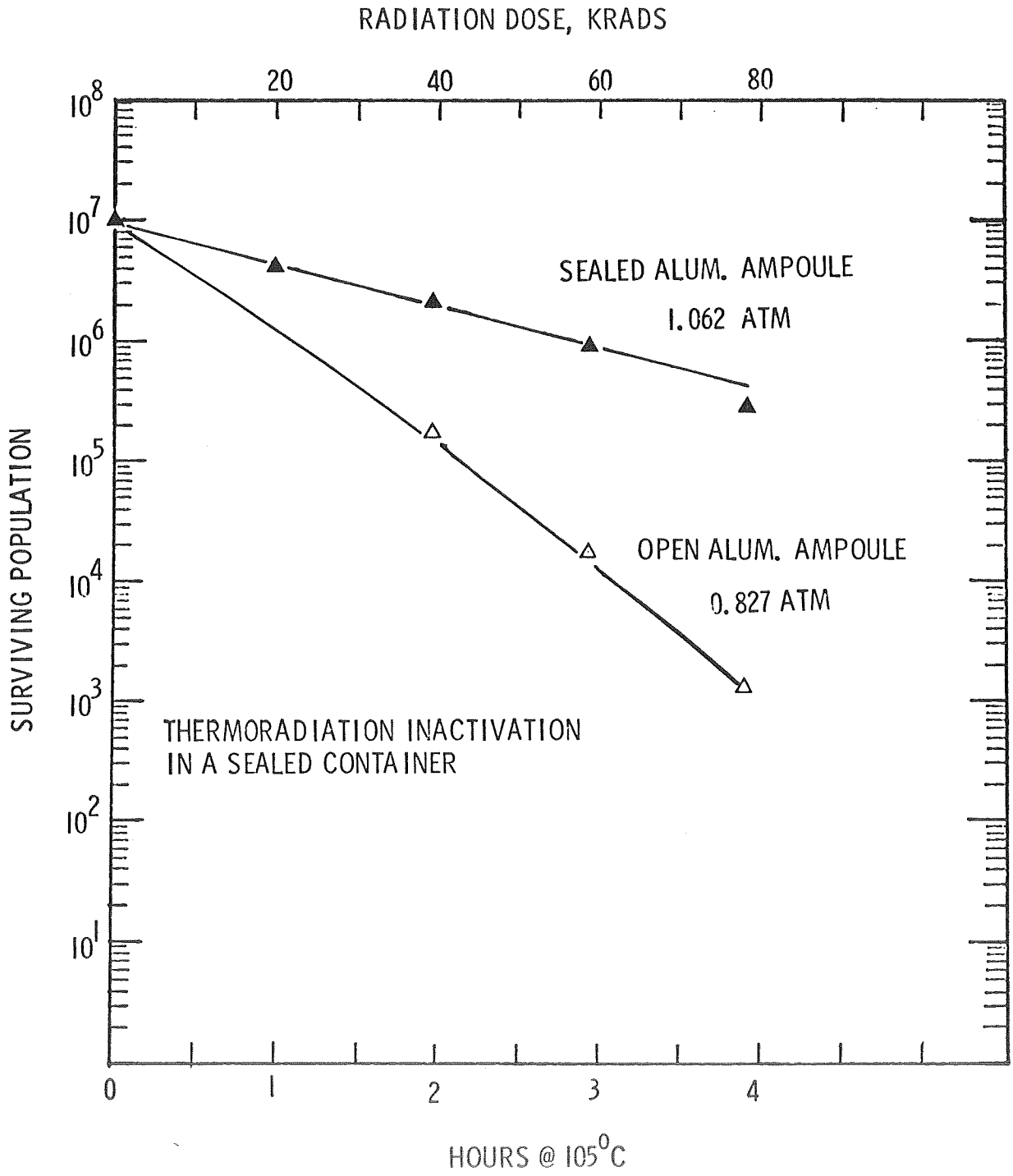
RADIATION DOSE, KRADS
20
40
60
80
10^8
10^7
10^6
10^5
10^4
10^3
10^2
10^1
SURVIVING POPULATION
SEALED ALUM. AMPOULE
1.062 ATM
OPEN ALUM. AMPOULE
0.827 ATM
THERMORADIATION INACTIVATION
IN A SEALED CONTAINER
0
1
2
3
4
HOURS @ 105°C

FIGURE 2

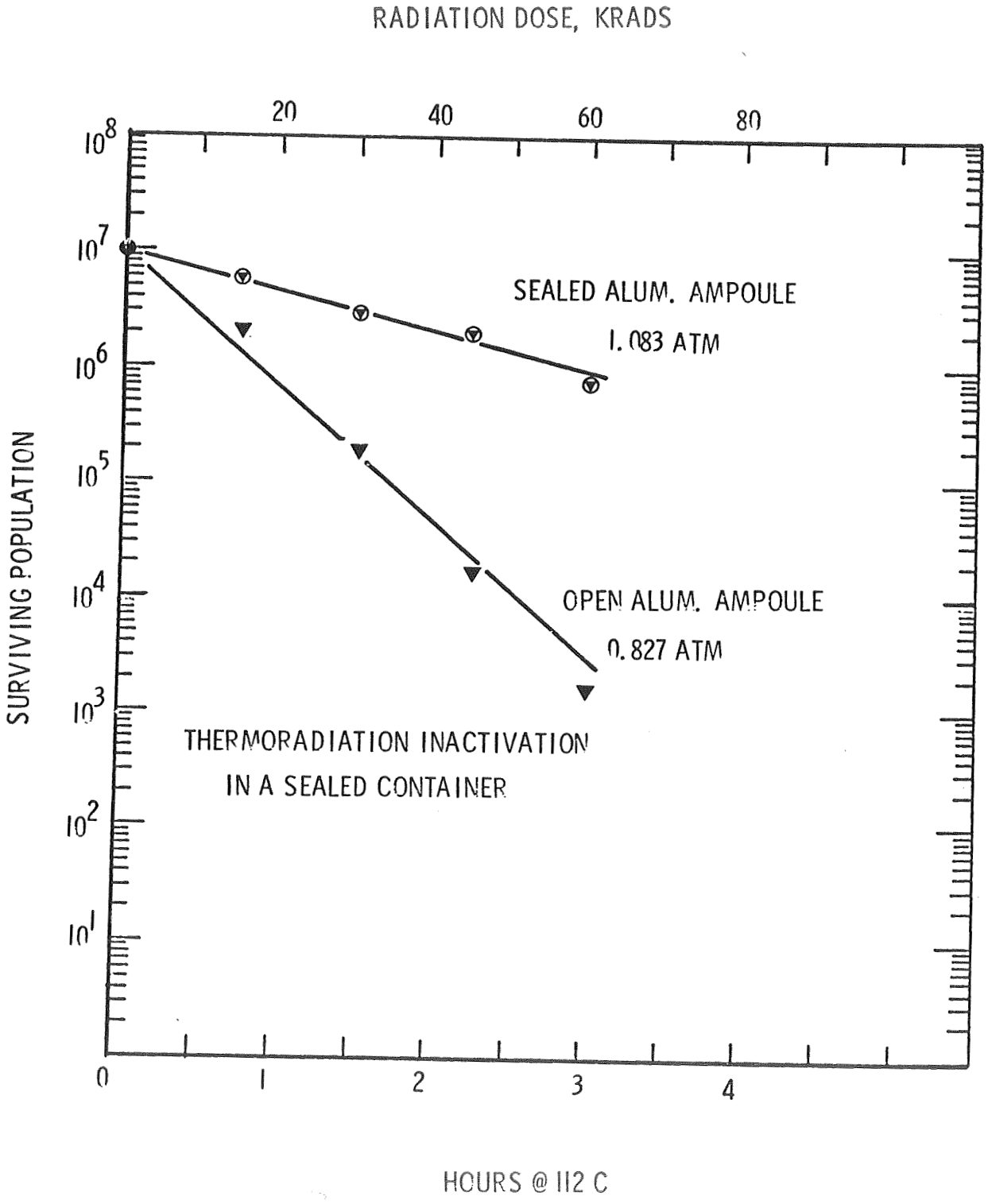
RADIATION DOSE, KRADS
20
40
60
80
10^8
10^7
10^6
10^5
10^4
10^3
10^2
10^1
SURVIVING POPULATION
SEALED ALUM. AMPOULE
1.083 ATM
OPEN ALUM. AMPOULE
0.827 ATM
THERMORADIATION INACTIVATION
IN A SEALED CONTAINER
0
1
2
3
4
HOURS @ 112 C

Figure 3

Preliminary Analysis of the Radiation Burden Of A Typical Mars Lander

A. Description. The objective of this activity is to provide a preliminary indication of the radiation dose which would be received by a typical Mars lander mission. This estimate can be used to help determine the maximum feasible radiation doses which can be used in any prelaunch spacecraft sterilization activity.

B. Progress. The first phase of this activity has been completed. This phase has been characterized by a gain in understanding of the sources and types of natural space radiations and by the completion of an estimate of the dose of each type of radiation for a twelve month travel time plus a maximum six month operational period on the planet's surface. A short discussion of these upper bound estimates is given below.

The six possible sources of radiation which will contribute to the accumulated dose of a Martian lander are: (1) particulate radiation (electrons and protons) trapped in the geomagnetic field, (2) galactic or cosmic radiation in the form of extremely energetic bare nuclei, (3) proton and alpha radiation from solar storms, (4) neutron and gamma radiation from radioisotope thermoelectric generators (RTG), (5) radiation released from the detonation of nuclear weapons, and (6) radiation used for spacecraft sterilization purposes. Provided there are no atmospheric detonations preceding or during the launch

of the spacecraft, item (5) will not be present. Therefore a survey of the first four items is necessary to form a basis for rationale concerning the use of item (6). A summary of these upper bound estimates of the spacecraft's interior components for years of solar maximum (years of greatest solar flare activity) and two different space shielding conditions are given in Table I and Table II.

TABLE 1

An Estimate of the Upper Bound on a Typical Mars Lander Mission Radiation Burden Assuming a Space Shielding of 1.0 gm/cm^2

Source of Radiation	Amount (RADS)
Geomagnetic Field (Van Allen)	42
Solar Flares	3000
Galactic Radiation	23
RTG Radiation (680 Thermal Watts)	
Neutrons	2120
Gamma	1130
Total	6315

TABLE 2

An Estimate of the Upper Bound on a Typical Mars Lander Mission Radiation Burden Assuming a Space Shielding of 10.0 gm/cm^2

Source of Radiation	Amount (RADS)
Geomagnetic Field (Van Allen)	13
Solar Flares	150
Galactic Radiation	23
RTG Radiation (680 Thermal Watts)	
Neutrons	2120
Gamma	1130
Total	3436

As has been stated, the total radiation doses described in Tables 1 and 2 are probably very liberal upper bounds since the estimate of the solar flare contribution is based upon rates during years of solar maximum, whereas the years of the middle 70's are years of solar minimum. During the years of solar minimum, the flare contribution for a 12 month trip with 1.0 gm/cm^2 shielding is approximately 400 rads, and the contribution with 10 gm/cm^2 shielding is only 20 rads. Using these expected flare doses, the total dose would be 3714 rads for 1.0 gm/cm^2 shielding. Hence, a conclusion which may be drawn is that the RTG will provide the largest share of the total radiation dose of any 18 month mission during the middle 1970's.

Humidity Control Systems

A. Description. Studies on spore inactivation as a function of relative humidity for fixed temperature has in general been done in closed systems. The tacit assumption has been that pressure effects under these conditions are negligible so that these studies closely approximate the actual effect of RH changes. There are reasons for questioning this assumption (QR 16 and 17). Therefore, it is desirable to carry out such studies in open systems. To this end humidity control systems which enable us to carry out inactivation studies in open systems are being developed.

B. Progress. Extensive modifications were made to the humidity control system which operates on the controlled saturation temperature concept (QR 17, p. 43). The capability of the system to furnish very dry air was extended greatly by pressurizing the saturation portion of the system and then adding a desiccant bed with controllable air flow-through. Each of these modifications and other changes are described separately below.

1. Pressurization of the System. The basic features of the original system were retained, but the saturator chamber in the warm water bath and the trap in the cold water bath were replaced with pressure vessels. Also, all plastic tubing was replaced with copper tubing and high pressure connections, and a pressure gage and valve were added (see Figure 1). In this way, the air can be completely saturated at any pressure up

to 6 atmospheres above ambient pressure and then expanded to ambient pressure with a predictable and controlled reduction in RH.

Since our laboratory is located at 5430 feet above sea level, the standard absolute air pressure is 12.2 psia. Assuming that ideal gas laws apply to water vapor and knowing the vapor pressures involved, the RH can be regulated by controlling the amount of pressure applied to the system. Therefore, the RH at any given saturation temperature can be reduced to one-half after expansion by adding one atmosphere of pressure. By increasing the pressure to two atmospheres (24.4 psig), the RH is reduced to 1/3 of the original value. Six atmospheres (73.2 psig) appears to be the practical limit for pressurizing the system, since the further addition of pressure yields only minimal reductions in RH. This relationship is illustrated in Figure 2.

The use of pressure in the system in effect provides a vernier control of RH between the lowest RH attainable at a given saturation temperature at ambient pressure and the RH attainable at the same temperature with six atmospheres pressure. For example, air saturated at 2°C will have an RH of about 27% at 22°C. When the system is pressurized to 73.2 psig, the RH is reduced to about 3.8% at 22°C.

2. Desiccant Bed. Even though the pressure greatly increased the low range RH capability, still lower RH values were needed for some of our dry heat sterilization experiments. Therefore, the system was further modified by adding a desiccant bed chamber with an adjustable bypass line.

When the desiccant bed is used, the relatively dry air from the pressurized portion of the system is expanded to ambient pressure and then passed through the desiccant before entering the temperature chamber. The bypass valve regulates the amount of air passing through the desiccant so that any portion or all of the 30 liters per minute airflow can be directed through the desiccant chamber.

This feature extends the low range RH capability from 3.8% at 22°C to 0.15% at 22°C. It is interesting to note that corresponding RH values at 105°C, a temperature frequently used in the dry heat experiments, are about 0.09% and 0.0035% respectively.

3. The RH temperature conversion chart (Figure 3) was extended downward from a saturation temperature of -16°C to -100°C. Dewpoint (saturation temperature) measurements are made periodically from samples of air entering the temperature chamber. This chart provides a convenient way to convert the dewpoint readings to RH at any temperature of interest and to verify calculated RH values. Further, it is used extensively as a tool to determine desired RH values at given temperatures in the design of experiments.

4. Temperature Chambers. Although the temperature chambers are not part of the humidity control systems per se, a chamber which admits ambient air can reduce the effectiveness of the humidity control. Therefore, the temperature chambers used both with the dry heat and thermoradiation experiments were dismantled, sealed, and reassembled. This sealing operation facilitates maintaining

a slight overpressure in the chambers and prevents the induction of ambient air.

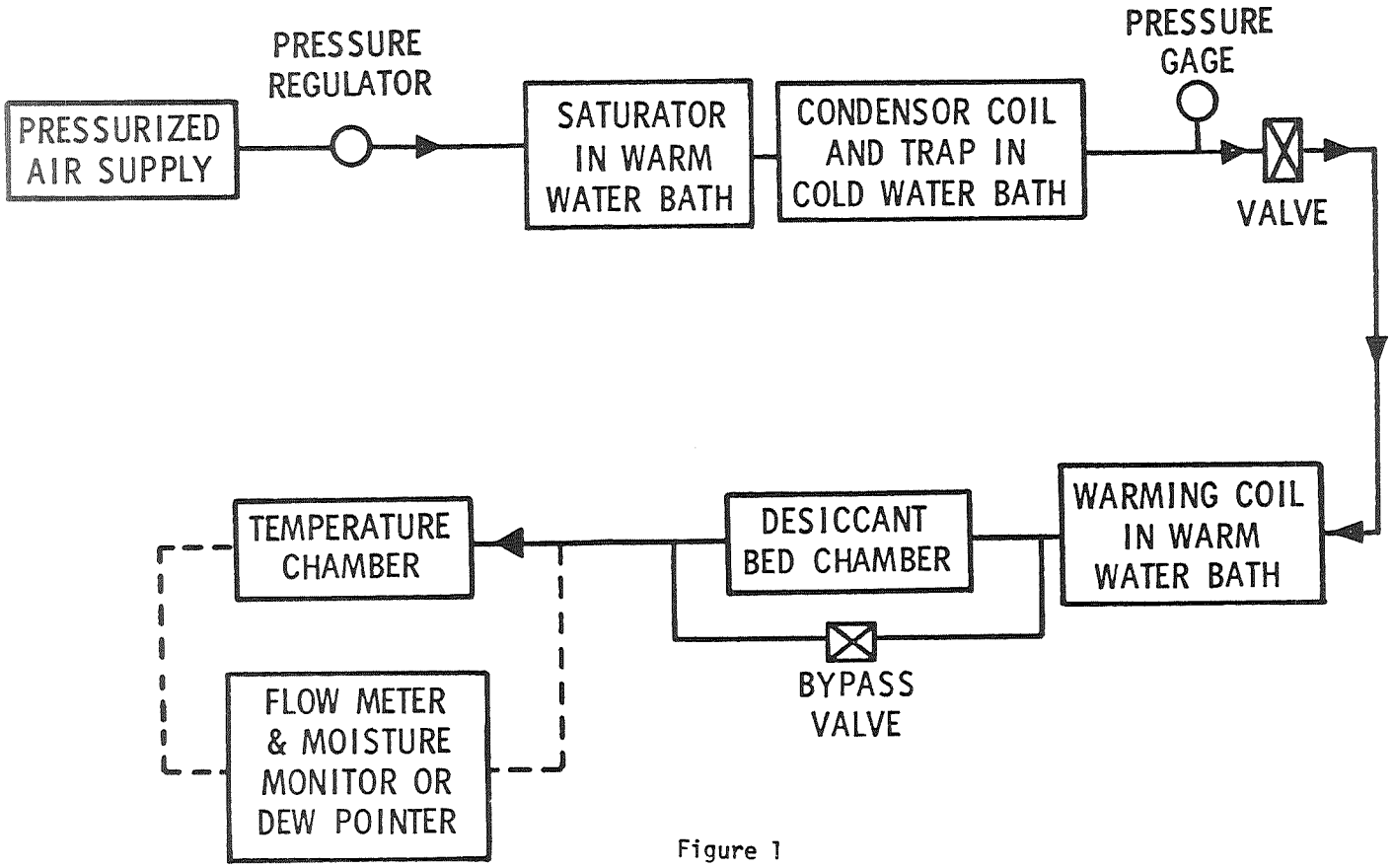
PRESSURIZED AIR SUPPLY
PRESSURE REGULATOR
SATURATOR IN WARM WATER BATH
CONDENSOR COIL AND TRAP IN COLD WATER BATH
PRESSURE GAGE
VALVE
WARMING COIL IN WARM WATER BATH
DESICCANT BED CHAMBER
BYPASS VALVE
TEMPERATURE CHAMBER
FLOW METER & MOISTURE MONITOR OR DEW POINTER

Figure 1

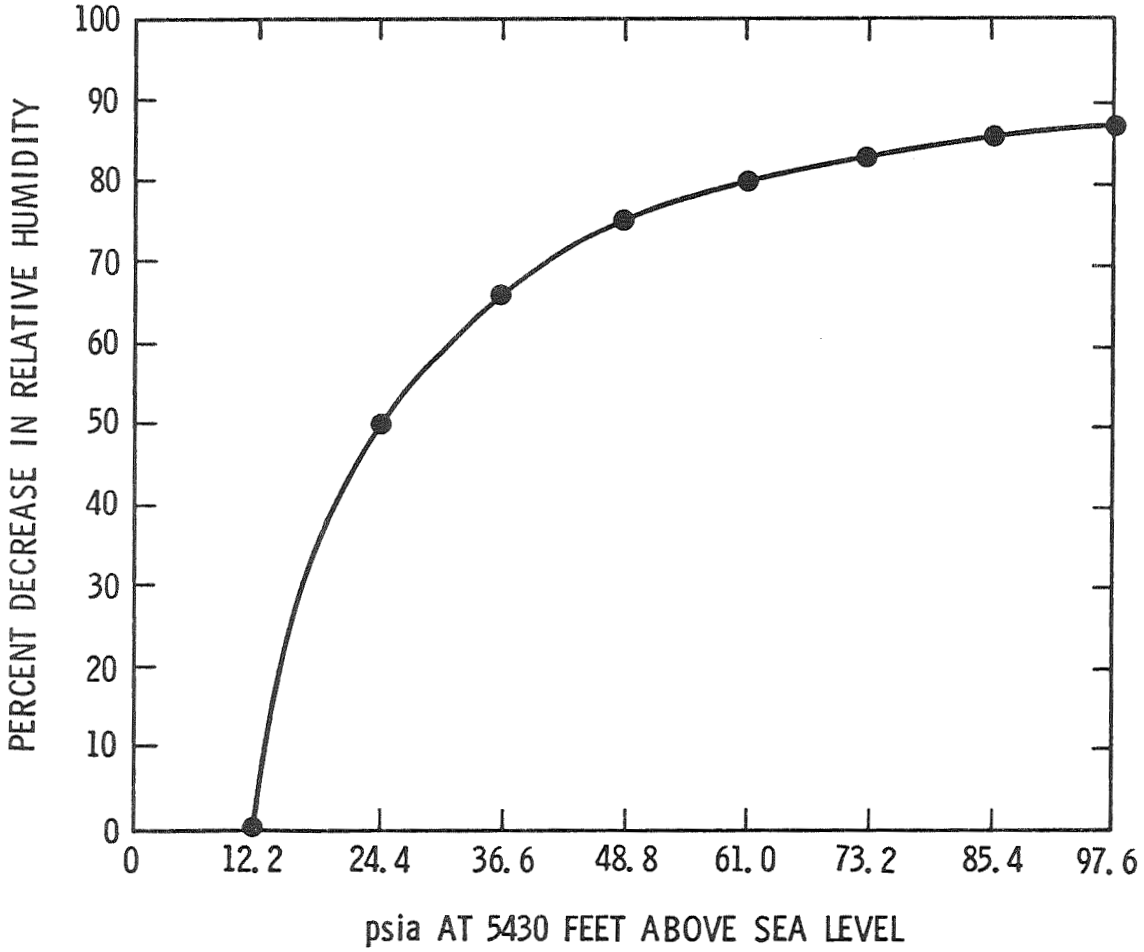
PERCENT DECREASE IN RELATIVE HUMIDITY
100
90
80
70
60
50
40
30
20
10
0
0
12.2
24.4
36.6
48.8
61.0
73.2
85.4
97.6
psia AT 5430 FEET ABOVE SEA LEVEL

Figure 2

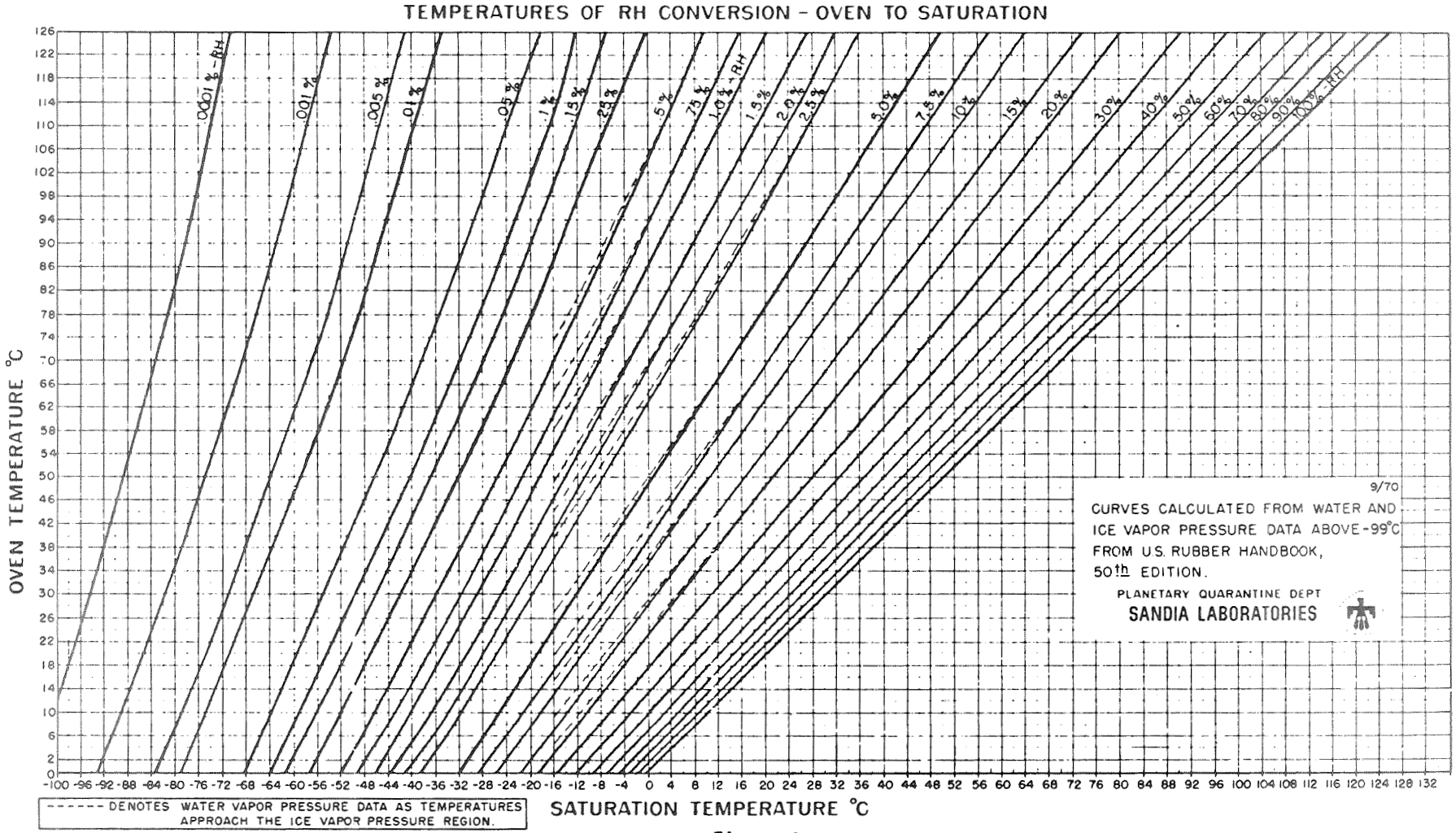
TEMPERATURES OF RH CONVERSION - OVEN TO SATURATION
OVEN TEMPERATURE °C
SATURATION TEMPERATURE °C
.0001 % - RH
.001 %
.005 %
.01 %
.05 %
.1 %
.15 %
.25 %
.5 %
.75 %
1.0 % - RH
1.5 %
2.0 %
2.5 %
3.0 %
7.5 %
10 %
15 %
20 %
30 %
40 %
50 %
60 %
70 %
80 %
90 %
100 % - RH
9/70
CURVES CALCULATED FROM WATER AND ICE VAPOR PRESSURE DATA ABOVE -99°C FROM U.S. RUBBER HANDBOOK, 50th EDITION.
PLANETARY QUARANTINE DEPT
SANDIA LABORATORIES
------ DENOTES WATER VAPOR PRESSURE DATA AS TEMPERATURES APPROACH THE ICE VAPOR PRESSURE REGION.

Figure 3

Bioburden Modeling and Experimentation

A. Description. In attempting to estimate or predict the bioburden on a spacecraft surface at any time t, the first estimate usually obtained is that of the expected (or mean) bioburden H(t) at that time. It must be remembered, however, that the probability that the actual burden exceeds this estimate of H(t) can be quite large. Thus, in order to be confident about sterilization procedures, one needs more information about the bioburden than just an estimate of the mean burden. It would be desirable to have a means of answering questions of the form: What is the probability that the actual burden exceeds twice the estimate of H(t), three times the estimate of H(t), ten times the estimate of H(t), and so forth? The only hope of obtaining such information is to have explicit knowledge of the quantities:

$P_j(t)$ = the probability that there are precisely j organisms on the surface of interest at time t, for j = 0, 1, 2, ...

Knowing this distribution of the number of organisms on the surface allows one to answer questions of the above form. Thus, for example, if the probability is sufficiently low that the actual burden exceeds ten times the estimate of H(t), sterilization cycles can be set for this ten-fold increase of the estimate knowing they will be in error with only a very small probability. Additionally, the choice of a two-, three-, or, say, ten-fold multiple of an estimated burden depends to some extent upon the number of samples taken in obtaining the estimate.

Thus, the more samples one takes, the more nearly the estimate of the expected bioburden coincides with the theoretical mean bioburden, thereby reducing the amount of subsequent compensation needed in answering questions of the above type. There is, therefore, some trade-off between this "compensating factor" (be it 2, 3, or 10) and numbers of samples. This trade-off can be analyzed only when the probabilities $P_j(t)$ are known--lending guidance for the establishment of sampling protocol.

From this, it seems reasonable that bioburden modeling, whether for estimation or prediction, should have as its aim the derivation of probabilities $P_j(t)$ representing the surface burden at time t. Parameters used to describe the $P_j(t)$ should be capable of being estimated from surface and/or environmental sampling data.

B. Progress. Since a model has been developed (see QR 15, 16,17) that is generally capable of meeting the above criteria, both as an estimation and a prediction model, the emphasis during this quarter has been on experimental verification of the model.

One approach being taken to verification is the following. The model may be summarized by the equations:

$$P_j(t) = \sum_{j=0}^{\infty} \frac{e^{-H(t)/\gamma} \cdot (H(t))^k}{k! \quad \gamma^k} Q(j,k), \qquad j=0, 1, 2, \cdots \qquad (1)$$

with

$$H'(t) = \gamma \cdot \lambda(t) - \mu(t)\, H(t) \qquad (2)$$

where

$H(t)$ is the mean number of organisms on the surface at time t,

γ is the mean number of organisms per clump

$\lambda(t)$ is the clump deposition rate

$\mu(t)$ is the clump removal fraction (that is, the removal rate is proportional to the number of clumps present, and $\mu(t)$ is the proportionality factor), and

$Q(j,k)$ is the probability that exactly j organisms reside on k clumps.

An experimental situation in which

(i) The particle removal fraction, $\mu(t)$

(ii) The particle deposition rate, $\lambda(t)$

(iii) The distribution of the number of microorganisms per particle, and

(iv) The number of microorganisms on a surface as a function of time,

may be independently controlled or measured first presents the possibility of verifying the relationships in equation (2). In this case, knowledge of (iii) allows γ to be calculated. Equation (2) may be solved for $H(t)$ as a function of γ, $\lambda(t)$, and $\mu(t)$. Thus the prediction for $H(t)$ (gotten from equation (2)) may be compared with direct estimates of $H(t)$. Should this lend confidence to the

validity of (2), one may proceed to verification of equation (1). Here, knowledge of (iii) allows one to calculate the Q(j,k)'s. Then knowledge of $\lambda(t)$, $\mu(t)$ and γ (condition (iii)) yields a predicted H(t) (equation (2)) and this in equation (1) yields a model prediction of the $P_j(t)$. These may be compared with the frequency distribution of numerous surface samples to determine if they are compatible.

It must be remembered that model verification is never an absolutely positive activity. Data disagreeing with the model appreciably implies a needed change in the model, but good agreement does not imply an absolute "correctness" of the model - only agreement "to date." The more agreement we obtain under as many conditions presumably compatible with the derivation of the model, the more confidence one may place in the model.

As previously reported, a facility in which the clump (particle) deposition rate may be controlled and measured has been developed. This is a vertical laminar-flow facility (VLF). Measuring and controlling the removal fraction and the distribution of the number of organisms per clump are the current major problem areas - and have been partially addressed this quarter. In addition, protocol for experimentation have been developed and some preliminary results with glass spheres have been obtained.

Particle Removal Fraction. Previous studies (QR 17) have shown that the air-flow in the VLF has a negligible effect upon particle removal when small glass spheres are deposited on glass slides. This quarter, attempts were made to use the vacuum probe in a subcritical mode to

effect a reasonably predictable removal fraction under these conditions. Glass slides (22 mm x 22 mm) were dusted with 0.1 gm of 10 μ glass spheres. These slides were then viewed microscopically, and the number of spheres were counted prior to any attempt at their removal. The slides were vacuumed using the vacuum probe operating subcritically at 2 psi across the filter membrane, and were then recounted. Figure 1 shows the results of these experiments as a plot of percent particles remaining versus the number of times the probe was passed across the slide. The data here were reasonably "rough" and an alternate means of achieving removal fractions in the range, say, 0.2 to 0.8 was sought.

The alternate means found was to vary the pressure drop across the membrane filter in the vacuum probe. Experimenting as above, this seemed to offer a better means of getting reliably predictable removal. Figure 2 shows the results of these experiments and indicates that this approach to removal is extremely promising.

Interaction Between Deposition and Removal of Particles Only in VLF.

The second set of experiments was designed to provide an environment where the deposition rate, removal fraction, and the number of particles present at each time t is measurable. Using the VLF (See QR 11) and the acoustic dust feeder (QR 10), a constant measurable environment was generated using 10 μ glass spheres. Glass slides were exposed to the environment for a given time. At predetermined intervals the slides were removed and the number of spheres on the slides are counted using a microscope. The slides are then partially cleaned using a vacuum probe in a subcritical flow rate condition as described above. The clean portions of the slides were then recounted, and the

slide was placed back in the same environment where the process was repeated.

The data and the analysis of the data from these experiments are not complete at this time. One can conclude, however, that a plateau is achieved. This situation may be likened to having one organism per clump. Generally, however, it will be necessary to actually tag these spheres with organisms to achieve the objectives outlined above.

Number of Microorganisms Per Particle with Mechanically Tagged Glass Beads. The purpose of the final experiment is to mechanically tag 10 μ glass beads and to determine the number of microorganisms per particle. These can then be used in experiments similar to that described above. This experiment can be viewed in two parts.

The first part consists of the particle preparation. Ten grams of 10 μ glass beads were mixed with 10 ml of a solution containing 10^9 Bacillus subtilis var. niger spores per ml.

The beaker containing the suspension was rotated in a 100°F oven for 24 hours. At the end of this time the particles had formed a solid dry layer on the bottom of the beaker. The layer was broken up slightly, but the particles were still in clumps. The particles were allowed to rotate for another 24 hours at 100°F. At the end of this time the particles were individuals with very few clumps being visible during a microscopic inspection.

The second part of this experiment involved the selection of the particles and their treatment to determine the distribution of the number of organisms per particle. A small quantity of the particles

were placed on a sterile glass slide. A 10% sterile sucrose solution was used to coat a sterile needle attached to a micromanipulator After drying for a few minutes, the needle was, of course, tacky. While being observed under a microscope, an individual glass bead was selected. The needle was lowered and the glass bead became attached to the needle. The needle with the particle attached was then removed. A small test tube filled with sterile sucrose solution was prepared and the end of the needle was immersed in the solution while it was being insonated. After 30 seconds the needle was removed and the tube was insonated for another 30 seconds to remove the microorganisms from the particle. The liquid was then added to a petri dish containing TSA and the place was counted after three days.

Preliminary data yield a mean number of three microorganisms per glass bead prepared in this manner with a standard deviation of 3.4.

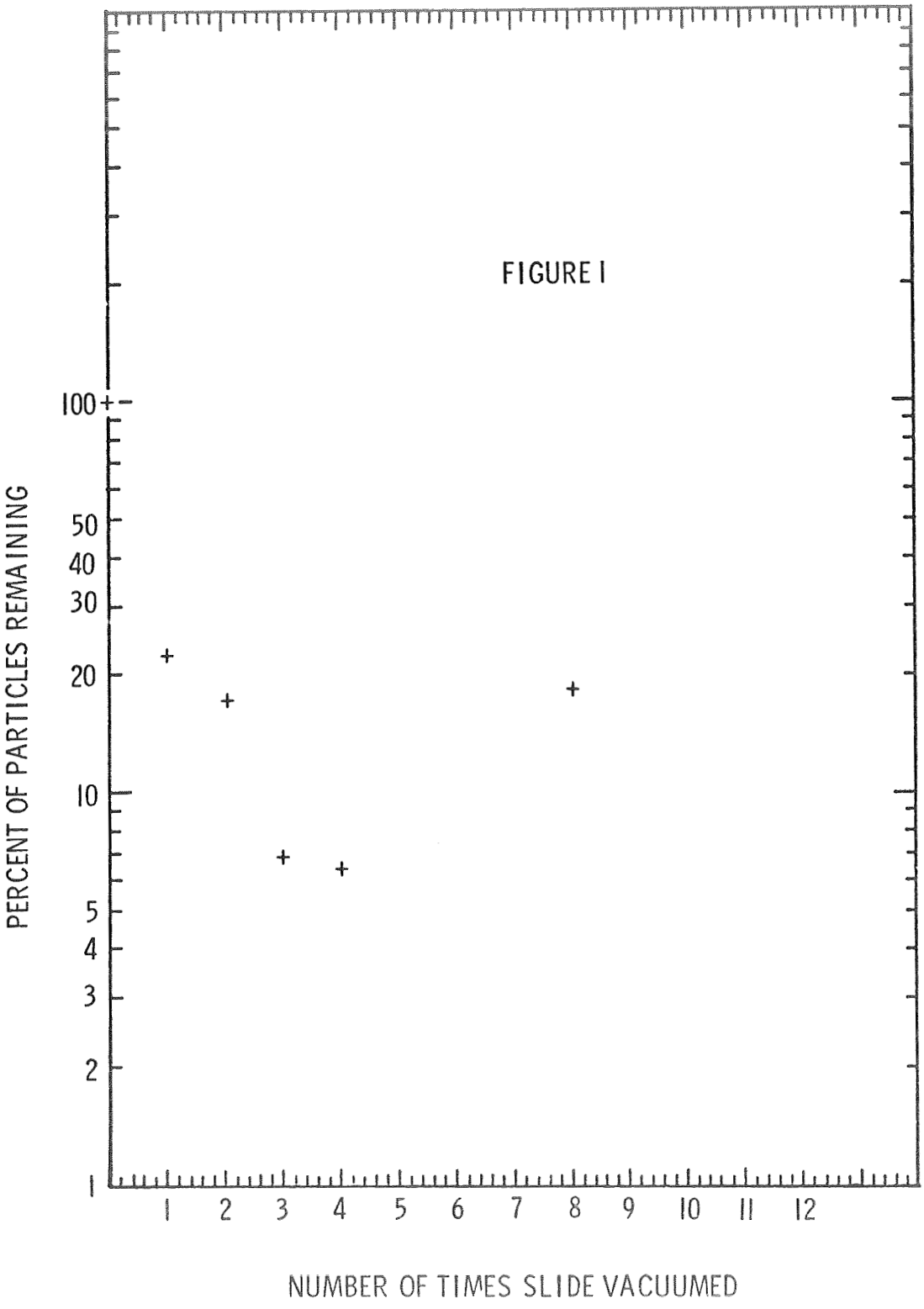
FIGURE I
PERCENT OF PARTICLES REMAINING
100
50
40
30
20
10
5
4
3
2
1
1 2 3 4 5 6 7 8 9 10 11 12
NUMBER OF TIMES SLIDE VACUUMED

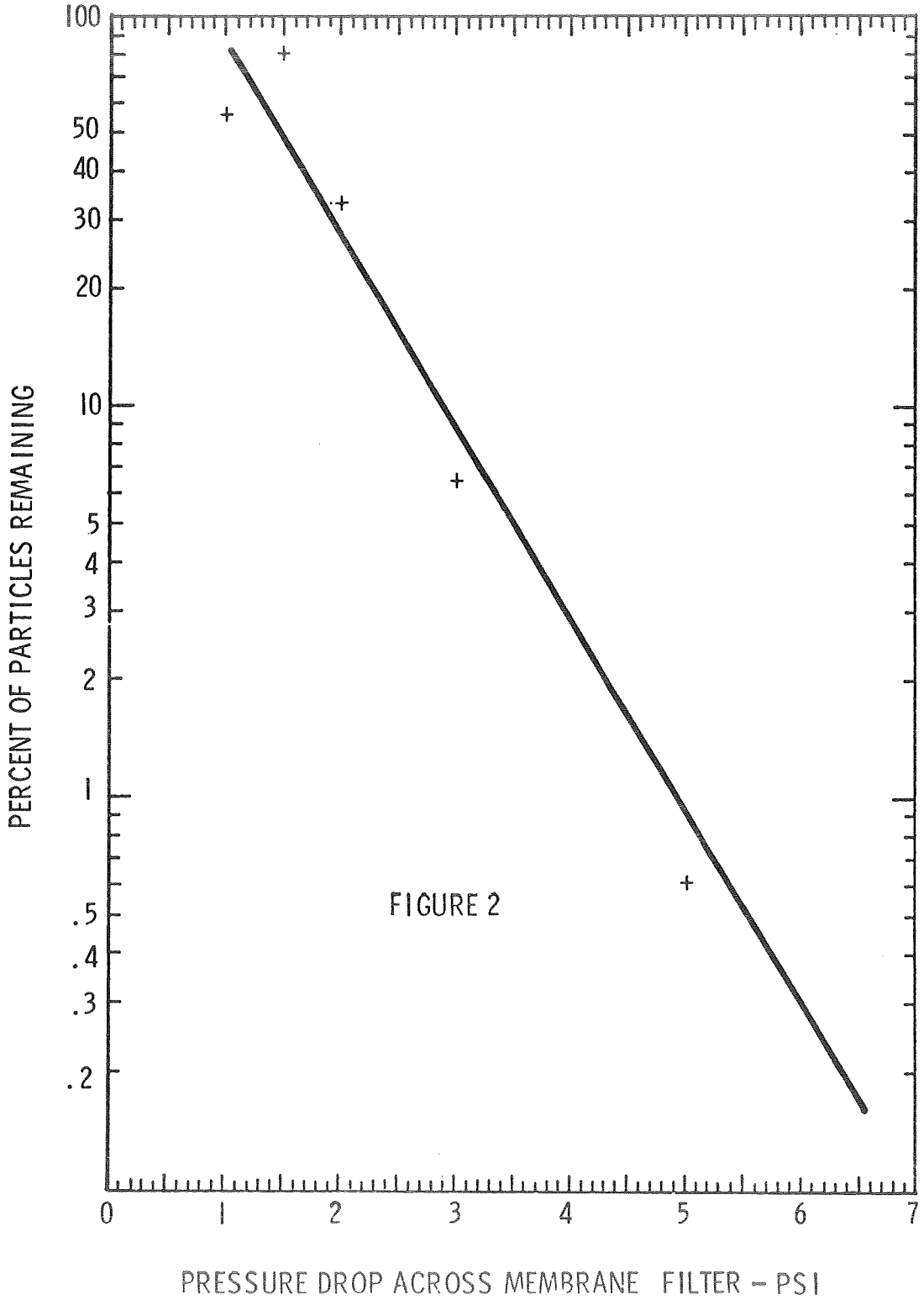
100
50
40
30
20
10
5
4
3
2
1
.5
.4
.3
.2
PERCENT OF PARTICLES REMAINING
0
1
2
3
4
5
6
7
PRESSURE DROP ACROSS MEMBRANE FILTER - PSI

FIGURE 2

Lunar Planetary Quarantine Information System

A. Description. The objective of this activity during this quarter was to develop the documentation for the users of the Planetary Quarantine Lunar Information System which now is being used at Cape Kennedy by the Public Health Service.

B. Progress. In an earlier quarterly report (OR 14) Sandia reported the completion of the

1. Problem Analysis
2. System Design
3. Systems Program, and
4. System Checkout

for the information system for lunar flights for the Planetary Quarantine Officer. During this quarter the last step in the overall program was completed.

Since the programs, as provided by Sandia, are being operated by not only the personnel of the U.S. P.H.S. at the Spacecraft Bioassay Laboratory at Cape Kennedy but also by the RCA personnel at the Real-Time Computer Facility (RTCS) at the Air Force Eastern Test Range, it is necessary that comprehensive information be provided as to how these programs are used. This documentation was completed during the present quarter.

The organization at RTCS has a standard format for the preparation of such documentation (see Real-Time Computer Systems Operating Procedure 5600 7.B.2). In preparing the documentation of the present system we have attempted to follow this guide when it

was feasible.

The titles of the chapters in this document are as follows:

1. Introduction
2. File Preparation Program (FILE)
3. Data Storage Program (DAST)
4. Qualitative Storage Program (QUAL)
5. Qualitative Summary Program (QUALSUM)
6. Lunar Inventory Program (LINT)
7. Reproduction Program (REPD)

A more complete description of the purpose of each of these programs may be found in previous quarterly reports.

Chapter 1 attempts to discuss the difference which exists between the system described in the original design (SC-RR-68-545) and the system as it now exists.

Chapter 2, and each of the succeeding chapters, has the following outline:

2.1 Purpose of Program

2.2 Input to Program

2.2.1 Control Data Deck

2.2.2 Run Data Deck

2.3 Output of Program

2.3.1 Error and Informative Messages

2.4 Models Used in the Program

2.5 Flow Diagrams of Program

2.6 Subroutines Used in the Program

2.7 Constants

2.8 Running Instructions

2.8.1 Necessary Peripheral Equipment

2.8.2 Loading Instructions

2.8.3 Typewriter Messages

Chapter 4 describes a revised version of QUAL which was also written during this quarter. This revision allows for modification of the identification scheme without requiring an extensive amount of reprogramming. Currently, identification is done by the PHS personnel at Cape Kennedy. This identification is stored in QUAL and is used in organizing qualitative microbial data by identification category in QUALSUM. A computerized identification scheme has been completed this quarter and may, if it is deemed desirable, be inserted into QUAL to perform the colony identifications automatically for use with QUALSUM. A separate document describing this work is in preparation.

Two final observations are appropriate. The information system document is written in a modular fashion so that changes may be instituted in the documentation as changes are made in the system. For example, should the automatic identification scheme be included in QUAL, Chapter 4 will be replaced.

The second observation is that this document is to be used in addition to SC-RR-68-545 not in place of it. Any definitions of terms given there are not repeated in the present work.

The information system documentation is in final preparation and should be available in the near future.

Publications

1. M. C. Reynolds, K. F. Lindell and N. Laible, "A Study of the Effectiveness of Thermoradiation Sterilization," SC-RR-70-423, June 1970.
2. M. C. Reynolds and D. M. Garst, "Optimizing Thermal and Radiation Effects for Bacterial Inactivation," Space Life Sciences 2(3) 1970.
3. J. P. Brannen, "Interim Report: Dry-Heat Sterilization Modeling," SC-RR-70-439, August 1970.
4. J. P. Brannen, "Microbial Sterilization in Ultra-High Vacuum and Outer Space: A Kinetic Comparison," Space Life Sciences, to appear.
5. J. P. Brannen, "An Anlysis of Vacuum Effects in the Sterilization of Microorganisms," Biophysik, to appear.
6. V. L. Dugan, "A Kinetic Analysis of Spore Inactivation in a Composite Heat and Gamma Radiation Environment," Space Life Sciences, to appear.

Presentations and Briefings

1. M. C. Reynolds, "Thermoradiation Sterilization," U. S. Army Medical Research and Development Command, Washington, D. C., August 11, 1970.
2. W. J. Whitfield conducted a session, "Laminar Flow Design and Special Application," as a faculty member at the University of Colorado, Boulder, Colorado on August 12, 1970.
3. H. D. Sivinski, "Laminar Air Flow in Planetary Quarantine," Xth International Congress for Microbiology, Mexico City, Mexico on August 14, 1970.

4. H. D. Sivinski, "Thermoradiation Sterilization and Its Applications," presented to Dr. Kurt H. Debus and his primary staff at Cape Kennedy, Florida on August 26, 1970.

Committee Activities

1. W. J. Whitfield, Member of a Public Health Service Committee to evaluate a grant request made by The Medical Research Center in Camden, New Jersey. A site visit was made to Camden on August 6, 1970. Expenses were paid by the Public Health Service.

Distribution:

NASA, Code SC
Grants and Contracts
400 Maryland Avenue, SW
Washington, D. C. 20546 (25)

L. B. Hall, NASA
Code SB
400 Maryland Avenue, SW
Washington, D. C. 20546 (25)

B. W. Colston
Director, Space & Special Programs
Division
Office of Operations
U.S. Atomic Energy Commission
Albuquerque, New Mexico 87115

L. P. Daspit, Jr.
Viking Project Quarantine Officer
Viking Project Office, NASA
Langley Research Center
Hampton, Virginia 23365

University of California, LRL
P. O. Box 808
Livermore, California 94551
Attn: Tech. Info. Div.
For: Report Librarian

Los Alamos Scientific Laboratory
P. O. Box 1663
Los Alamos, New Mexico
Attn: Report Librarian

Richard G. Bond
School of Public Health
College of Medical Science
University of Minnesota
Minneapolis, Minnesota 55455

John H. Brewer
Star Route 2
Brownwood, Texas 76801

Edward B. Kasner
Director of Research Services
Graduate College
University of New Mexico
Albuquerque, New Mexico

Frank B. Engley, Jr.
Chairman, Department of Microbiology
School of Medicine
University of Missouri
Columbia, Missouri

Gilbert V. Levin
Biospherics, Inc.
4928 Wyaconda Rd.
Rockville, Maryland 20853

Irving J. Pflug
Professor of Environmental Health
University of Minnesota
College of Medical Sciences
Minneapolis, Minnesota 59455

Gerald Silverman
Department of Nutrition and Food Science
Massachusetts Institute of Technology
Cambridge, Massachusetts 02139

John A. Ulrich
School of Medicine
University of New Mexico
Albuquerque, New Mexico

Samuel Schalkowsky
Exotech Incorporated
525 School Street, SW
Washington, D. C. 20024

Boris Mandrovsky
Aerospace Technology Division
Library of Congress
Washington, D. C.

Mark A. Chatigny
Research Engineer
Naval Biological Laboratory
Naval Supply Center
University of California, Berkeley
Oakland, California 94625

Richard G. Cornell
Associate Professor of Statistics
Department of Statistics
Florida State University
Tallahassee, Florida

Martin S. Favero
Department of Health, Education
and Welfare
CDC-Phoenix Field Station
4402 North 7th Street
Phoenix, Arizona 85014

Mr. James Martin
Viking Project Engineer
Langley Research Center, NASA
Langley Station
Hampton, Virginia 23365

Q. Ussery
Code NC3, Quality Assurance Branch
Manned Spacecraft Center, NASA
Houston, Texas

F. J. Beyerle
George C. Marshall Space Flight Center
Manufacturing Engineering Laboratory
Code R-ME-MMC
Huntsville, Alabama 35812

J. Gayle
Code SOP
Kennedy Space Center,NASA
Cape Canaveral, Florida

Murray Schulman
Division of Biology and Medicine
Headquarters, AEC
Washington, D. C. 20545

N. H. MacLeod
Space Biology Branch
Code 624, Bldg. 21, Rm. 161
Goddard Space Flight Center
Greenbelt, Maryland 20771

J. E. Campbell
U. S. Public Health Service
222 E. Central Parkway
Cincinnati, Ohio 45202

G. Rotariu
Process Radiation Staff
Division of Isotopes Development
Headquarters, AEC
Washington, D. C. 20545

Martin G. Koesterer, Microbiologist
Bioscience Operation
General Electric
P. O. Box 8555
Philadelphia, Pennsylvania 19101

Carl Bruch
Chief, Bacteriology Branch
Division of Microbiology
Food and Drug Administration
3rd & C.,S.W.,Room 3876
Washington, D. C. 20204

John W. Beakley
Department of Biology
University of New Mexico
Albuquerque, New Mexico

Loren D. Potter, Chairman
Department of Biology
University of New Mexico
Albuquerque, New Mexico

Loris W. Hughes
Department of Biology
New Mexico State University
University Park, New Mexico

Richard W. Porter
Corporate Engineering Staff
General Electric Company
570 Lexington Avenue
New York, New York

Fred L. Whipple
Smithsonian Astrophysical Observatory
Cambridge, Massachusetts 02138

J. J. McDade
Biohazards Group
Pitman-Moore Company
Dow Chemical Company
P. O. Box 10
Zionsville, Indiana 46077

Otto Hamberg
Aerospace Corporation
Building A2, Room 2019
2350 East El Segundo Blvd.
El Segundo, California

Lawrence P. Chambers
NASA Headquarters
Office of Manned Space Flight
Code MLR
Washington, D. C. 20546

Arthur H. Neill
Code SB
400 Maryland Avenue, SW
Washington, D. C. 20546

Richard Green
Jet Propulsion Laboratory
4800 Oak Grove Dr.
Pasadena, California 91103

Rudy Puleo
Public Health Service
Spacecraft Bioassay Laboratory
Drawer Y
Cape Canaveral, Florida 32900

USAEC, Division of Technical
Information
P. O. Box 62
Oak Ridge, Tennessee 37830
Attn: Reference Branch
P. E. Postell

Carl Sagan
Cornell University
Center for Radiophysics and Space
Research
Space Science Building
Ithaca, New York 14850

Document Library
Lovelace Foundation for Medical
Education and Research
5200 Gibson Blvd. SE
Albuquerque, New Mexico 87108

Martin S. Tierney
Group J-10
Los Alamos Scientific Laboratory
Los Alamos, New Mexico

E. C. Pollard
Professor of Biophysics
Pennsylvania State University
618 Life Sciences Building
University Park, Pennsylvania 16802

Robert Angelotti
Deputy Director
Division of Microbiology
Food and Drug Administration
Health, Education and Welfare
200 C. Street SW
Washington, D. C. 20546

Vance I. Oyama, Chief
Life Detection Systems Branch
NASA, Ames Research Center
Moffett Field, California 94035

Byron W. Brown, Jr.
Department of Community and
Preventive Medicine
Stanford University School of Medicine
Stanford University Medical Center
Stanford, California 94305

Don G. Fox
Sterility Control Officer
NASA Headquarters, Code SB
400 Maryland Avenue SW
Washington, D. C. 20546

A. A. Rothstein
Manager, Planetary Quarantine
Martin Marietta Corporation
Mail No. 8401
Denver, Colorado 80201

Hillel S. Levinson
U. S. Army Natick Laboratory
Natick, Massachusetts

B. S. Schweigert, Chairman
Department of Food Science
College of Agriculture
Michigan State University
East Lansing, Michigan 48823

H. O. Halvorson
Biochemistry Department
St. Paul Campus
University of Minnesota
St. Paul, Minnesota

Jack Kaye
11607 Georgetowne Court
Patomic, Maryland 20854

A. Anellis
U. S. Army Natick Laboratories
Natick, Massachusetts

H. W. Johnson, LTC
U. S. Army Medical Research and
Development Command
Washington, D. C. 20314

Donald A. Kautter
Dept. of HEW
Food and Drug Administration
Div. of Microbiology
BF-135
200 C Street S. W.
Washington, D. C. 20204

Dr. Richard C. Corlett
Dept. of Mechanical Engineering
University of Washington
Seattle, Washington 98105

J. A. Hornbeck, 1
J. M. Wiesen, 100
W. J. Howard, 1000
D. B. Shuster, 1200
W. A. Gardner, 1500
H. E. Lenander, 1600
T. M. Burford, 1700
C. Winter, 1710
D. R. Morrison, 1720
J. W. Worrell, Jr., 1721
D. P. Peterson, 1724
R. G. Clem, 1730
H. D. Sivinski, 1740 (35)
A. A. Lieber, 1750
R. W. Henderson, 2000
C. B. McCampbell, 2310
B. H. Van Domelen, 2345
S. J. Buchsbaum, 5000
L. C. Hebel, 5200
A. W. Snyder, 5220
R. M. Jefferson, 5221
J. E. McDonald, 5300
L. M. Berry, 5500
D. W. Ballard, 7361
L. S. Ostrander, 8232
G. A. Fowler, 9000
J. H. Scott, 9200
A. Y. Pope, 9300
L. A. Hopkins, Jr., 9500
R. S. Gillespie, 3411
J. L. Gardner, 3422
Calla Ann Crepin, 3424-1

hev